Development of a Magnetic Intra-Uterine Manipulator

by

Stefan Doll

Thesis presented in partial fulfilment of the requirements for the degree of Master of Science in Mechatronic Engineering at Stellenbosch University

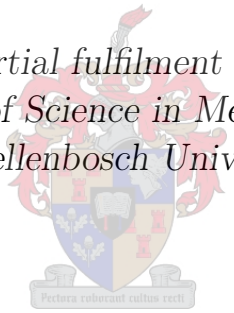

Department of Mechanical and Mechatronic Engineering,
University of Stellenbosch,
Private Bag X1, Matieland 7602, South Africa.

Supervisor: Prof. C. Scheffer

March 2012

Declaration

By submitting this thesis electronically, I declare that the entirety of the work contained therein is my own, original work, that I am the owner of the copyright thereof (unless to the extent explicitly otherwise stated) and that I have not previously in its entirety or in part submitted it for obtaining any qualification.

Signature: .....
S. Doll

Date: March 2012 .....

Abstract

Development of a Magnetic Intra-Uterine Manipulator

S. Doll

Department of Mechanical and Mechatronic Engineering,
University of Stellenbosch,
Private Bag X1, Matieland 7602, South Africa.

Thesis: MScEng (Mechatronic)

March 2012

Uterine manipulation is integral to obtaining adequate access to the uterus during a laparoscopic procedure. A variety of mechanical manipulators have been developed to aid the surgeon with the dissection of the uterus during laparoscopic hysterectomies. Limitations of existing manipulators are that they require an additional assistant during surgery, are expensive and may cause tissue trauma to the vaginal or cervical canal. This study introduces the novel concept of a magnetic uterine manipulator, intended to overcome existing devices' shortcomings and enabling non-invasive uterine manipulation. The first goal of the study was to investigate the strengths and weaknesses of existing mechanical manipulators and compare them to those of a magnetic device. Analysis showed that a magnetic manipulator would not be able to compete in terms of the range of motion of existing devices. A limited anterior-sagittal rotation range of 60° was seen in the magnetic manipulator compared to a range of 140° in mechanical devices. However, the magnetic manipulator could eliminate the need for an extra assistant, is reusable and thus also more economical. The second goal was to investigate which type of setup would be most successful at effective uterine manipulation. Through concept analysis a cart-on-arch system was deemed most effective. To lift an effective load of 1 N over an air-gap of 150 mm rare-earth N38 Neodymium (NdFeBr) magnets showed the most promise as magnetic actuators. FEA (Finite Element Analysis) simulations of the magnetic setup were validated experimentally which produced an acceptable MAE (mean absolute error) of 0.15 N. Furthermore, a comparative simulation study of shielded and unshielded magnets was done which concluded that shielded magnets produce a slightly higher attraction force and would be safer to use due to less magnetic flux fringing. Thirdly and lastly, potential safety hazards and risks of using magnetic actuators in surgical

environments were identified. The literature research revealed that connections between magnetic fields and health risks to patients have not been conclusively proven in clinical studies to date, but nonetheless, great care should be taken in situations where the patient has a pace-maker or orthopaedic implants, as these might interact with the magnetic field. Recommendations for future work include further research into the geometry and scaling effects of magnetic shielding as well as electromagnetic actuator design. Electromagnetic actuators could replace rare-earth magnets, if coil and cooling systems are optimized, resulting in magnets that can be reversed or switched off and which are therefore easier to control and safer to handle.

Uittreksel

Ontwikkeling van 'n Magnetiese Intra-Uteriene Manipuleerder

("Development of a Magnetic Intra-Uterine Manipulator")

S. Doll

Departement Meganiese en Megatroniese Ingenieurswese,
Universiteit van Stellenbosch,
Privaatsak X1, Matieland 7602, Suid Afrika.

Tesis: MScIng (Megatronies)

Maart 2012

Baarmoedermanipulasie is van uiterste belang om sodoende voldoende toegang te kry tot die baarmoeder gedurende 'n laparoskopiese prosedure. Daar is reeds 'n verskeidenheid meganiese manipuleerders ontwikkel as hulpmiddel vir die chirurg in die ontleding van die uterus tydens laparoskopiese histerektomies. Beperkings van bestaande manipuleerders is dat 'n bykomende assistent tydens chirurgie benodig word. Die manipuleerders is ook duur en kan weefseltrauma veroorsaak aan die vaginale of servikale kanale. Die studie stel 'n nuwe konsep bekend: 'n magnetiese baarmoedermanipuleerder, gemik daarop om bestaande toestelle se tekortkominge te oorkom en nie-indringende baarmoedermanipulasie moontlik te maak. Die eerste doel van die studie was om die voordele en nadele van bestaande meganiese manipuleerders te ondersoek en dit te vergelyk met dié van die magnetiese toestel. Analise het getoon dat 'n magnetiese manipuleerder nie met bestaande toestelle sal kan kompeteer waar dit gaan om beweegruimte nie. Daar is 'n beperkte anterior-sagitale rotasiespeling van 60° in die magnetiese manipuleerder, terwyl die meganiese toestel 'n rotasiespeling van 140° het. Die magnetiese manipuleerder kan egter die nodigheid van 'n bykomende assistant uitskakel, is herbruikbaar en dus ook meer ekonomies. Die tweede doel van die studie was om die tipe opstelling wat meer suksesvol sal wees tydens doeltreffende baarmoeder manipulasie te ondersoek. Konsep-analise het getoon dat 'n "cart-on-arch"stelsel die beste sal werk. N38 Neodimium (NdFeBr) magnete het die beste vertoon as magnetiese aandrywer om 'n werklike belasting van 1 N oor 'n lugspasie van 150 mm te lig. EEA (Eindige Element Analise) simulasies van die magnetiese opstelling is

eksperimenteel bekragtig en het 'n aanvaarbare gemene absolute fout (GAF) van 0.15 N gelewer. 'n Vergelykende simulasie studie het verder gewys dat beskutte magnete 'n effens hoër aantrekkingskrag oplewer en sal dus veiliger wees om te gebruik vanweë die verminderde magnetiese stromingsrand. Derdens en laastens is potensiële veiligheidsrisikos en gevare in die gebruik van magnetiese drywers in chirurgiese omgewings geïdentifiseer. Literatuurnavorsing het onthul dat die verband tussen magneetvelde en gesondheidsrisikos aan pasiënte nog nie voldoende bewys is in kliniese studies tot op datum nie. Gevalle waar pasiënte 'n pasaangeër of ortopediese inplantings het moet met groot sorg hanteer word aangesien dit dalk kan reageer met die magneetvelde. Aanbevelings vir toekomstige werk sluit verdere navorsing in in die rigting van die geometrie en die afskilferingseffek van magnetiese beskutting en ook elektromagnetiese drywer ontwerp. Elektromagnetiese drywers kan moontlik rou aarde magnete vervang indien winding en afkoelstelsels ge-optimeer word wat kan lei tot magnete wat omgekeer of afgeskakel kan word en dus makliker beheerbaar is en veiliger om te hanteer.

Acknowledgements

I would like to express my sincere gratitude to the following people and organisations:

- Professor Cornie Scheffer for his guidance and faith in the project.
- My Parents for there undying support and belief in me.
- My fellow BERG members for their support and the necessary coffee breaks.

Dedications

I would like to dedicate this thesis to my parents who have always believed in me. I'm very grateful for your support. To my darling Kari, thank you for the hours spent reading through every word. I would not have made it without your love and your ability to pick me up when things got difficult. Thank you.

Contents

List of Figures

List of Tables

Nomenclature

Constants

g	Gravitational Constant = 9.81	[m/s^2]
μ_0	Permeability of Free space = $4\pi\times\ 10^{-7}$	[dimensionless]

Variables

B_r	Remnance	[T]
$B_{x_{cube}}$	Flux Density of cube at distance x	[T]
$B_{x_{cyl}}$	Flux Density of cylinder at distance x	[T]
d	Distance	[m]
F	Force	[N]
H_c	Coercivity	[A/m]
i	Current	[A]
l	Length	[m]
M	Moment	[Nm]
m	Mass	[kg]
N	Number of turns	[Turns]
R	Radius	[m]
R_f	Feedback Resistor	[Ω]
R_s	Source Resistor	[Ω]
V_{in}	Voltage in	[V]
V_{out}	Voltage out	[V]
x	Distance from point	[m]
χ	Susceptibility	[dimensionless]
μ_r	Relative Permeability	[H/m]
∇	Curl of a vector field	[m]

Vectors

$\mathbf{A}$	Magnetic Vector Potential	[V $\cdot$ s/m]
$\mathbf{B}$	Flux density vector	[T]

H	Magnetic Field Intensity	$[\mathrm{A-turn/m}]$
J	Current Density	$[\mathrm{A/m^2}]$
M	Magnetization	$[\mathrm{A/m}]$

Abbreviations & Definitions

AH	Abdominal Hysterectomy
emf	Electromagnetic Flux
EPM	External Permanent Magnet
FEA	Finite Element Analysis
IPM	Internal Permanent Magnet
LAVH	Laparoscopically Assisted Vaginal Hysterectomy
LH	Laparoscopic Hysterectomy
MagLev	Magnetic Levitation
NdFeBr	Neodymium Iron Boron
TLH	Total Laparoscopic Hysterectomy
VH	Vaginal Hysterectomy

Anteversion	an abnormal position of an organ in which it is tilted or bent forward on its axis, away from the midline
Catheterization	to introduce a catheter into
Coercivity	the magnetic-field strength necessary to demagnetize a ferromagnetic material that is magnetized to saturation
Colpotomy	a surgical incision into the wall of the vagina
Endometrium	the mucous membrane lining of the uterus
Epithelium	the cellular covering of internal and external surfaces of the body
Insufflation	the act of blowing a powder, vapour, or gas into a body cavity

Isthmus	the constricted part of the uterus between the cervix and the body of the uterus
Laparoscopy	a minimally invasive procedure in which tiny incisions are made around the naval area for tool and camera insertion which is normally followed by a surgical procedure
Myometrium	the muscular wall of the uterus
Permeability	the degree to which a material is penetrable by a magnetic field
Remanance	the ability of a material to retain magnetization after the removal of a magnetizing field
Retroversion	an abnormal position of an organ in which it is tilted or bent backward on its axis, away from the midline
Stereotaxis	a surgical technique that uses medical imaging to precisely locate in three dimensions an anatomical site to which a surgical instrument or a beam of radiation is directed
Suprapubically	situated, occurring, or performed from above the pubis
Susceptibility	the degree to which a material can support the formation of a magnetic field

Chapter 1

Introduction

1.1 Background

A hysterectomy is a procedure where either part of or the entire uterus is removed from the female reproductive tract. Around 1 000 000 hysterectomies are performed annually worldwide (Mettler *et al.*, 2010). To put that number into perspective, roughly 900 000 cardiac surgeries are performed worldwide within the same time frame (Wijeysundera *et al.*, 2010). An ever increasing number of these hysterectomies are being performed laparoscopically nowadays. This type of operation is a minimally invasive procedure where miniature incisions are made in the abdominal wall. Ports are then inserted into these incisions through which the surgeon has access to the abdomen. The surgery is performed with tools inserted through the ports and viewed on an LCD screen via an abdominal camera. Laparoscopies limit external scarring, reduce patient recovery time, reduce tissue trauma in the patient and are generally less invasive than the conventional norm which are abdominal hysterectomies. Unfortunately, a laparoscopic hysterectomy is much more complicated than an abdominal hysterectomy, where the uterus can easily be visualized and manipulated through the incision in the abdomen. This means more intricate tools are required in the already expansive array of laparoscpic surgical equipment. The critical factor in laparoscopic surgery is being able to manipulate the uterus as extensively and as easy as possible to gain access to surrounding tissue which needs to be dissected from the uterus. A variety of uterine manipulators have been developed for this purpose, where most of them cover essentially the same design of a cervically inserted manually controlled actuator. These designs generally work well but do require the presence of an assistant to operate the manipulator. An easy to use and less expensive system that can be operated by only one surgeon would thus be of great benefit to surgeons and patients alike.

1.2 Primary Objective and Motivation

The primary objective of this study is the development and critical evaluation of a uterine manipulator that is actuated magnetically. A question that might be posed is: Why the need for a magnetic uterine manipulator? There are several reasons. Firstly, existing uterine manipulators pose a rather crude, albeit functional solution for uterine manipulation. Most manipulators have a very similar design, with a flexible tip, an extension shaft and the manipulator handle as depicted in Figure 1.1. Use of a manipulator during surgery requires insertion of the manipulator through the vagina into the cervical canal and lodging the tip in the uterus itself. The manipulator remains in the vaginal and cervical canal for the duration of the surgery. In addition to the discomfort caused by the hysterectomy, the patient often experiences tissue trauma inflicted unintentionally by trying to position the manipulator correctly in the cervix. Due to the huge number of hysterectomies performed yearly worldwide, there is an even greater need to ensure the safety and well-being of the patients undergoing these surgeries.

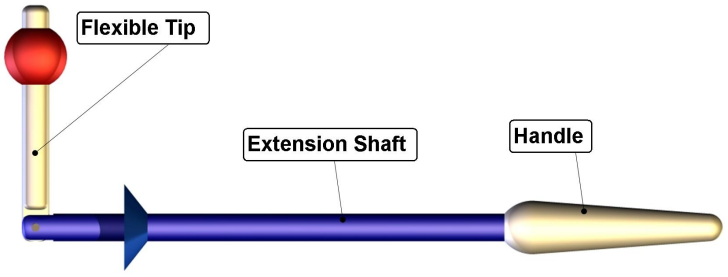

Figure 1.1: Example of a Mechanical Uterine Manipulator

Secondly, existing uterine manipulators are rather expensive, ranging from \$390 - \$2500. Many of these are not reusable either, adding to the already high surgery costs of between \$6000 - \$15000, according to Sculpher *et al.* (2004). This makes the prospect of using a simple grasper or forceps for manipulation more attractive, which in turn have the disadvantage of taking up an extra laparoscopic port.

Lastly, most uterine manipulators require an extra assistant during surgery to operate the manipulator. This limits space in the theatre and again raises the total cost of the operation. Research into the development of a magnetic intra-uterine manipulator therefore creates a promising concept for a surgical tool that is easy to use, patient and surgeon friendly and makes effective use of the limited theatre space.

1.3 Problem Statement and Research Questions

The most obvious benefit of using a magnetic uterine manipulator is the lack of a crude mechanical manipulator that has to be inserted into the uterus cervically and has to be operated by an extra assistant. It is however not certain how strong a magnet would have to be to be able to manipulate the entire uterus to a degree where it would be useful during surgery. Secondly, the strength of the magnet is directly related to its dimensions, thus even if the magnet was strong enough for uterine manipulation, its size might render it impractical due to space limitations in the operating theatre. Thirdly, there are a range of different magnets available and comparative research has to be done to determine what type of magnets would be best suited as manipulators. Lastly, it is unclear what the safety hazards of strong magnets in a surgical environment are. Consequently four research questions were formulated for this study:

- How does a magnetic uterine manipulator compare to a mechanical uterine manipulator?
- What type of mechanical setup is best suited for magnetic manipulation?
- Which type of magnets are best suited for magnetic uterine manipulation?
- What potential safety hazards could a magnet pose in a surgical environment and how can these risks be diminished?

1.4 Scope

The following section gives an outline of the study activities as well as the content of this report.

1.4.1 Research Activities

The research done on this thesis was divided into distinct phases which, individually, played an integral part in the completion of this thesis. The research comprised of a literature review, a conceptual design, modelling and validation of the final concept, testing of a prototype and finally, report writing. The literature review took approximately six months to complete and consisted of research in the area of magnetic/human interaction, particularly in the surgical environment. Further, research was done on large air-gap magnetic problems and Finite Element (FE) modelling of magnetic problems, especially with the

FE solver MagNET by Infolytica. The concept design phase included identifying all the key parts that would have to be combined to be able to build an operational prototype. The design and modelling phase comprised the majority of the time spent on the project and included adapting the research from the literature study to practical use. The design comprised simple empirical and analytical analysis before moving on to FE modelling of the magnetic problem. Furthermore, designs went through several iterations and design validations before a decision was made to build the prototype.

The testing phase was performed after completion of the prototype to make sure it adhered to all the design parameters. Lastly, the reporting phase spanned more or less the entire project, running parallel to the other activities. The research was completed after a timespan of approximately 18 months. Future work should include a cadaver study to test the prototype under simulated conditions of a real hysterectomy.

1.4.2 Document Outline

Chapter 2 provides an overview of the literature study results. The study covered the anatomy of the uterus as well as an in depth study into existing manipulators. Existing magnetic systems for surgery were researched extensively to cover ground on possible concepts. Lastly, the literature study also features magnetic theory, which was necessary to fully understand and model the research problem.

Chapter 3 summarizes the conceptual designs that were made toward the prototype. Concepts for the external magnet, the internal magnet and the actuator were conceived and analysed according to their strengths and weaknesses.

Chapter 4 covers the in depth design and modelling of the chosen concepts. Initial magnetic design was done using equations derived from Maxwell's Electromagnetic Theory to gain some insight into the problem and the dimensions involved. Emphasis was then put on the Finite Element (FE) modelling using Infolytica's MagNET software. Furthermore, model verification had to be performed to test the validity of the FE design. This section also covers the motor selection and actuator design.

Chapter 5 summarizes the testing of the final prototype. Force measurement to determine the attractive force between the magnets was done using a high sensitivity load cell. In addition, the actuator was tested for range of motion. This chapter also summarizes the entire design.

Chapter 6 concludes the study by summarizing the report and discussing the outcomes of the study. Insights into the design, and shortcomings thereof are discussed, and recommendations are given for future work on this topic. Finally the implications of research into magnetic manipulators for future surgeries are discussed.

Chapter 2

Literature Review

This chapter presents the result of a literature study on the different fields associated with uterine manipulation. The first section contains information about the anatomy of the uterus and the review of the procedure during a hysterectomy. The second part of the study focusses on magnets in the field of health science.

2.1 Anatomy of the Uterus

The uterus is a pear shaped female reproductive organ about 7.5 cm in length with a maximum diameter of 5 cm. It typically weighs 30 - 40 g and is stabilized by a various ligaments. The organ consists of two regions: the *body* and the *cervix*. The *body* is the largest division of the uterus. The *fundus* is the rounded portion of the body superior to the attachment of the uterine tubes. Furthermore the *body* ends at a constriction known as the *isthmus*. The *cervix* is the inferior portion of the uterus and projects a short distance into the vagina, while the uterine cavity opens into the vagina at the external orifice, or *cervical os* (Martini *et al.*, 2000).

The uterine wall is made up of an inner endometrium and a muscular myometrium. These layers are covered by the perimetrium, which is a layer of visceral peritoneum. The endometrium of the uterus includes the epithelium lining the uterine cavity and the underlying connective tissues. In adult women of reproductive age, and who have not given birth, the uterine wall is about 1.5 cm thick (Martini *et al.*, 2000). The uterus is supplied with oxygenated blood via the uterine artery. Figure 2.1 depicts the anatomy of the uterus.

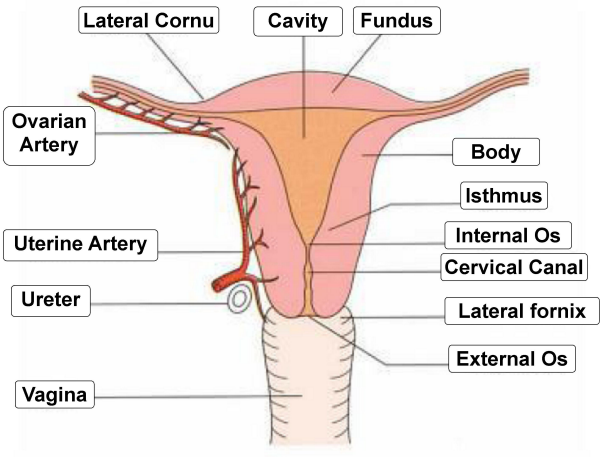

Figure 2.1: Anatomy of the Uterus in the Coronal plane (Image: (Ellis and Mahadevan, 2010))

The uterus is bent forward at the level of the *internal os* at an angle of 170°, this is called *antiflexion* of the uterus. If the cervix tips backwards to form an angle of 90° with the longitudinal axis of the vagina the orientation is called *antiversion* of the uterus. Thus, the uterus lies in almost a horizontal plane in the body. In some cases the cervical axis can be orientated upwards and backwards, this is termed *retroversion* of the uterus. If the uterine axis is orientated upwards and backwards, this is termed *retroflexion* (Ellis and Mahadevan, 2010). Figure 2.2 represents the different orientations of the uterus in the female body.

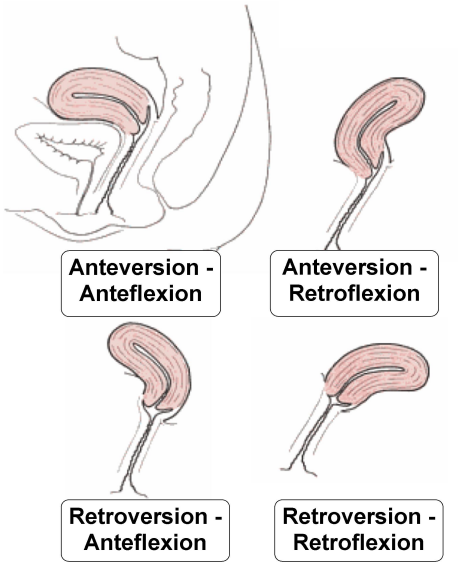

Figure 2.2: Orientation of the Uterus as seen in the Sagittal plane (Image: (Ellis and Mahadevan, 2010))

2.2 The Hysterectomy

The term hysterectomy comes from the Greek words *hystera*, meaning "womb", and *ektomia*, meaning "a cutting out of". This type of operation was first performed abdominally in 1843, by Charles McDowell in Manchester, England, but unfortunately ended with the patient dying in the immediate post-operative period (Sutton, 1997). Today, thanks to the introduction to anaesthesia, antisepsis and antibiotics, the mortality rate of a hysterectomy was lowered from a staggering 90% to 0.086%. During a successful total hysterectomy the patient's uterus *body*, *fundus* and *cervix* as well as surrounding connecting tissue are removed, either through the vagina or through the peritoneum.

2.2.1 Types of Hysterectomies

After the first successful hysterectomy in Lowell, Massachusetts, in 1853 by Ellis Burnham, the procedure was further developed by a number of American and European surgeons to the standard it is at today. Different methods of performing hysterectomies were researched, mainly for the purpose of lowering patient recovery time, decreasing tissue trauma and lowering theatre time and costs. These methods of accessing and removing the uterus can be subdivided into three main categories, mainly abdominal hysterectomies, vaginal hysterectomies and laparoscopic hysterectomies (Sutton, 1997).

In an abdominal hysterectomy (AH) an incision is made into the lower abdomen and the surgeon can then locate and access the uterus through this incision. The uterus is then separated and removed via the incision.

A vaginal hysterectomy (VH) involves the uterus being separated and removed exclusively via the vaginal canal. This procedure is exclusively utilized for patients with smaller uteri. The advantages of this procedure are the lack of visible scars as well as a shorter recovery time. On the other hand the procedure is quite complicated and requires a skilled surgeon.

The last type of procedure is a laparoscopic hysterectomy (LH). It involves the surgeon making tiny incisions into the lower abdomen of the patient and inserting surgical tools through them with which the uterus will be separated and removed. A camera is inserted via one of the incision ports so that the surgeon can visualize the operation. After separation of the uterus from the surrounding tissue, the organ is removed through the cervical and vaginal canal (Mettler *et al.*, 2010).

During the course of this report the focus will lie on total laparoscopic hysterectomies (TLH) and laparoscopic assisted vaginal hysterectomy (LAVH) as these procedures strongly rely on external uterine manipulators to manoeuvre the uterus. Figure 2.3 depicts the extent of reproductive organ removal for different types of procedures.

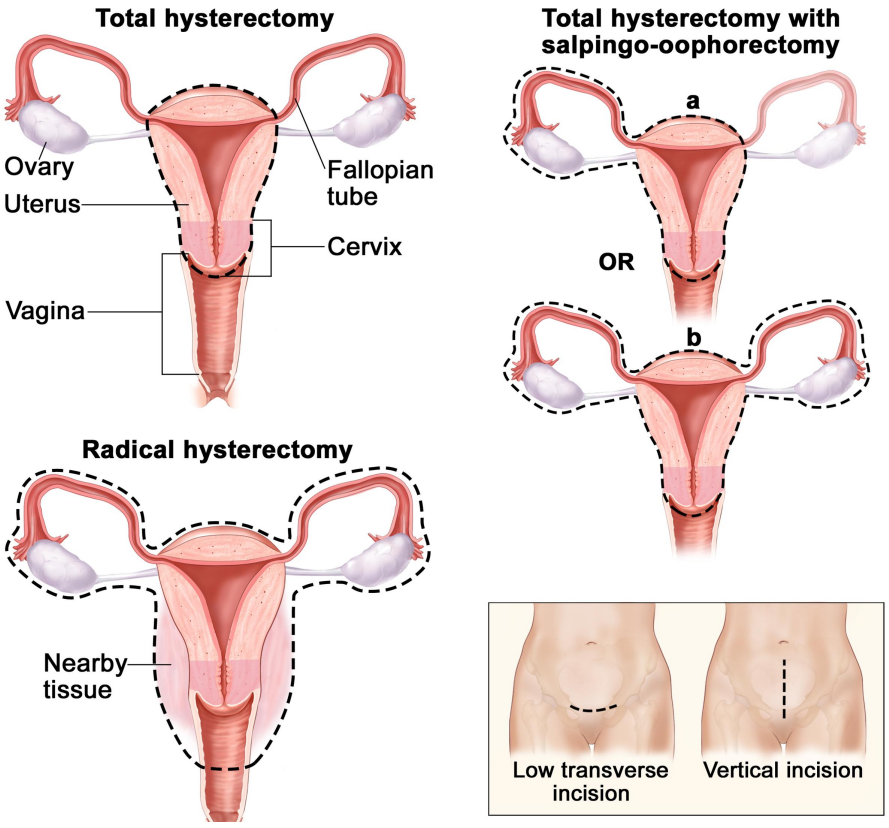

Figure 2.3: Organ removal during different types of hysterectomies (Image: Gyrus ACMI)

2.2.2 Procedure of a Laparoscopic Hysterectomy

During a laparoscopic hysterectomy tiny incisions are made into the lower abdomen of the patient. Ports are then inserted into these incisions which facilitate the introduction of surgical tools into the lower abdomen. Figure 2.4 depicts the location and size of the incisions.

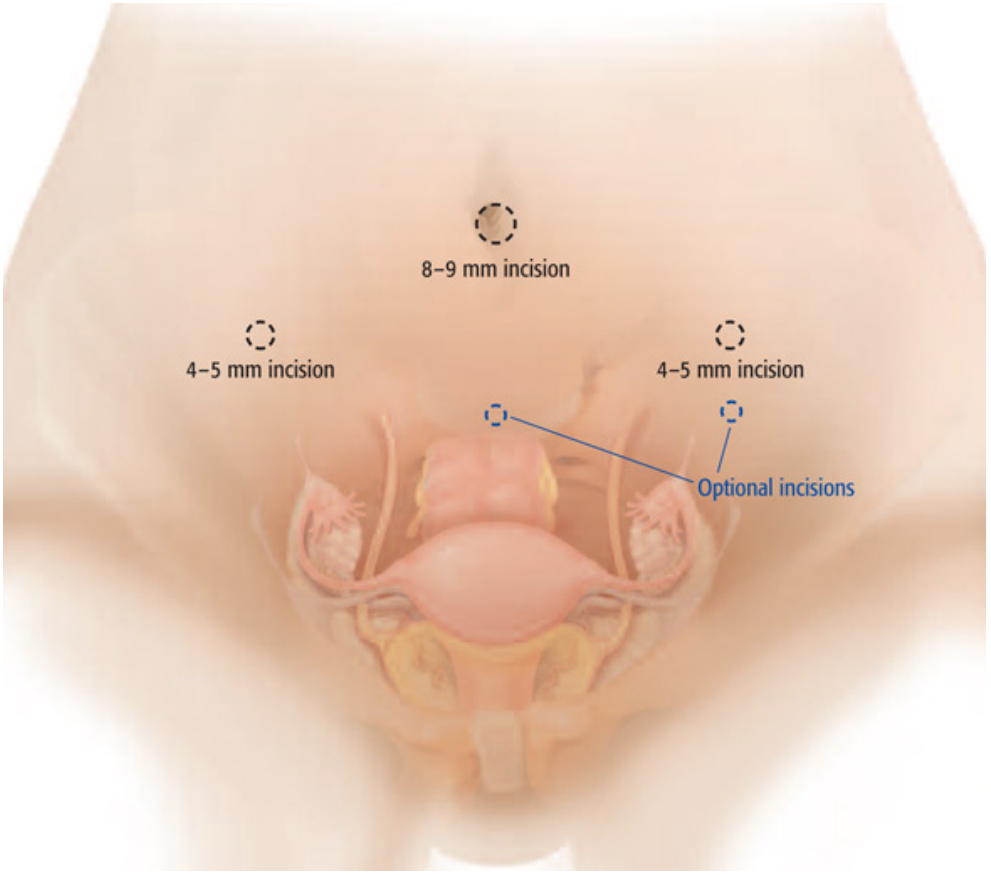

Figure 2.4: Incisions in a Laparoscopic hysterectomy (Image: Gyrus ACMI)

There are three major incisions made into the patient's abdomen. The umbilical incision serves as access for the umbilical port which in turn is used for insufflation of the abdomen and after is used as access for the laparoscope. After insufflation of the abdomen to a pressure of 12 - 15 mm Hg, the laparoscope is inserted into the umbilical port. The pelvis and abdomen are visually inspected and after a positive result the left and right lower lateral ports are inserted. Said ports are used for the insertion of graspers and other laparoscopic instruments, for example ligation and cauterizing devices. In most cases a fourth incision is made *midline suprapubically* to aid in dissection and manipulation (Covens and Kupets, 2009). At this stage the uterine manipulator is inserted into the uterus via the cervix. Elkington and Chou (2006) outline the rest of the procedure as follows:

- Division of the round ligaments
- Division of ovarian ligament or infundibulo-pelvic ligament

- Reflection of bladder off the cervix
- Uterine artery pedicles
- Colpotomy
- Specimen retrieval
- Vault closure

During surgery anteversion and retroversion, as depicted in Figure 2.2, are positions that allow ultimate access for uterine dissection. Consequently, modern uterine manipulators put great emphasis on being able to manipulate the uterus in this way and thus this thesis will also focus on being able to achieve the desired ranges of manipulation.

2.2.3 Comparison of Uterine Manipulators

As mentioned in Section 2.2.1, uterine manipulators are essential in performing a laparoscopic hysterectomy. These tools come in various shapes and sizes, but a common factor is that they are all inserted into the uterus cervically and have to be operated by an assistant. Some manipulators may even act as colpotomizing cups once the uterus is dissected. Table 2.1 lists the most popular uterine manipulators in the industry and attempts to compare them according to various factors that play a role in manipulator selection. This table will be used as a benchmark for the system developed in this thesis.

A generalization of the "perfect" uterine manipulator is depicted in Figure 2.5. This image depicts the combined maximum range of movement of all manipulators listed in Table 2.1. Refer to Appendix A for an explanation of the anatomical planes used in the description of rotational movement.

Table 2.1: Comparison of Uterine Manipulators Adapted from Mettler and Nikam (2006)

Manipulator	Movement			Reusable	Maintenance	Independant Movement	Ease of Assembly	Cost
	Anteversion / Retroversion	Lateral	Elevation					
Clermont-Ferrand	140°	130°	140°	Yes	✓✓✓	✓✓✓✓	✓	±$2500
Hohl	130°	90°	140°	Yes	✓✓	✓✓✓	✓	±$8500
Endopath	130°	90°	140°	No	✓✓	✓	✓✓	N/A
RUMI with Koh-cup	140°	90°	140°	Partially	✓✓✓	✗	✓	±$395
Hourcabie	90°	140°	140°	Yes	✓	✓✓✓✓	✓✓✓	N/A
Vcare	90°	90°	140°	No	✓✓✓	✗	✓✓✓✓	N/A
TLH-Dr Mangeshikar	130°	90°	140°	Yes	✓✓✓	✓✓	✓✓✓	±$2500
ClearView	170°	130°	140°	No	✓✓	✓✓	✓	N/A
Cohen Cannula	140°	130°	140°	No	✓✓✓	✓	✓✓	±$345

✗ = "Not Applicable", ✓= "Slightly Applicable", ✓✓= "Moderately Applicable", ✓✓✓= "Applicable",✓✓✓✓= "Very Applicable"

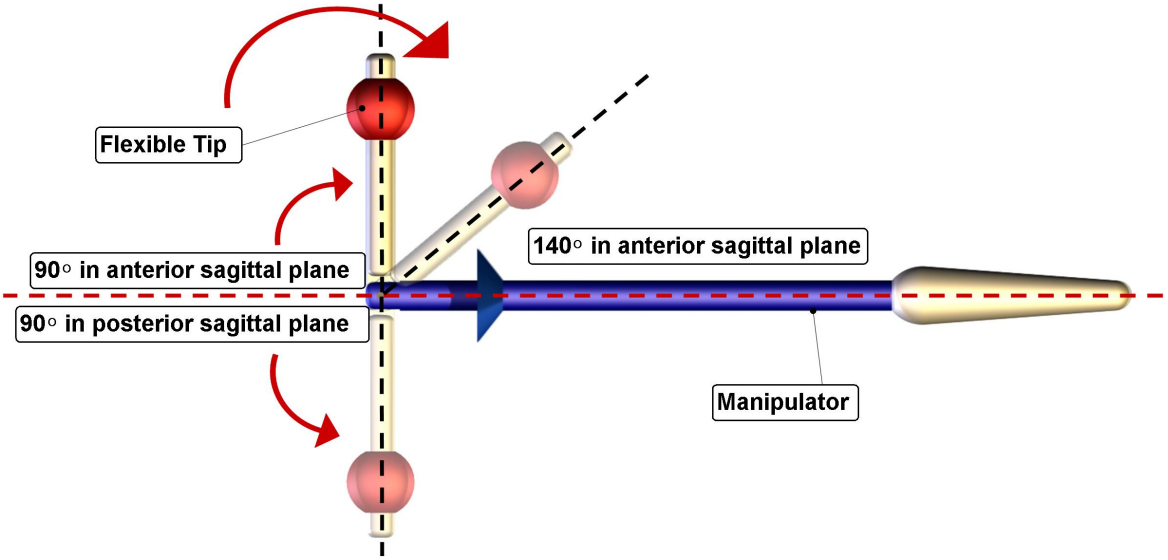

(a) Front view of manipulator rotation capability

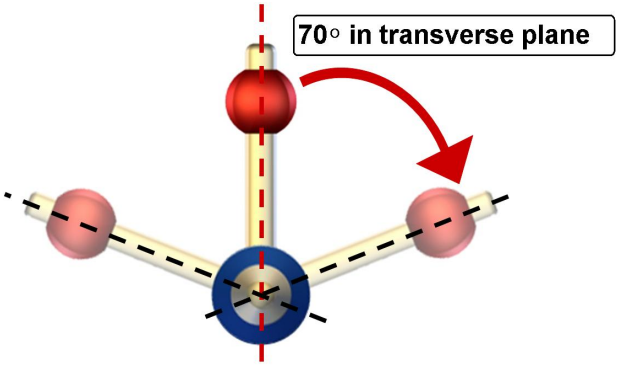

(b) Side view of manipulator rotation capability

Figure 2.5: Manipulator Rotation Capability

2.3 Magnets in Medicine

Magnets, or then known as lode stones, first came to human attention at around 1200 BC. This coincided with the event of bringing smelted iron in close contact with iron oxide (Fe_3O_4). Little was known about these mysterious stones and only in 1289 Petrus Peregrinus went about documenting well known, but then inexplicable, magnetic properties namely, magnetic forces act over a distance; secondly, similar poles repel unlike poles attract; thirdly, only magnetic materials are attracted by magnets and finally, north poles point to Earth's magnetic north (Andrä and Nowak, 1998).

The uses of magnets for medicine were first discovered by a Hindu surgeon, Sucruta, around 600 BC (Andrä and Nowak, 1998). In his texts he describes the use of magnets to extract arrow tips from his patients. These ideas were not

explored further for almost two millennia, from whereon the use of magnets has steadily become more popular to be included in various healing, anchoring and visualization techniques during operations or recovery. Figure 2.6 describes the use of magnets for medicine

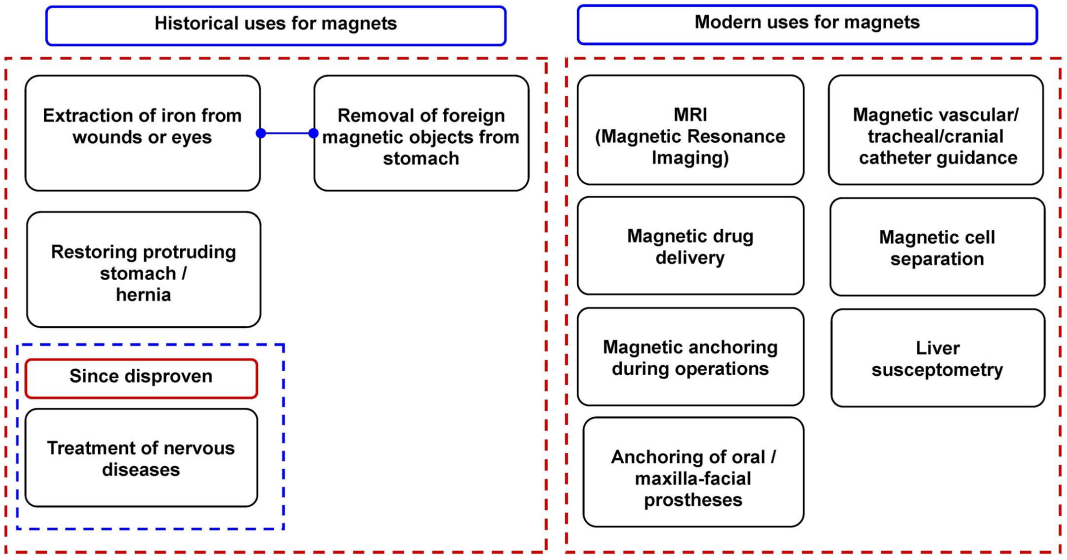

Figure 2.6: Historical and Modern uses for Magnets in Medicine

Today's technological advances and the invention of superconducting electromagnets have opened up a broad avenue for research into magnetics. The following subsections will delve deeper into specific uses of magnets in medicine regarded as being relevant guidelines and research for the completion of this study.

2.3.1 Medical Uses of Magnets as Manipulators or Anchors

Magnets have found a wide range of uses in modern surgery and patient recovery. This thesis focusses on magnetic manipulation and anchoring and thus the scope of research was narrowed down to the latter two topics. Boeckler *et al.* (2008) describe the use of micro rare-earth permanent magnets as anchors for removable oral prostheses. These devices are very small, ranging from 3 - 5.5 mm in diameter. They are able to achieve pulling forces of up to 5.8 N and aid in retention of the prostheses during chewing and have proven very successful. Further successful experimental uses for magnets as anchors have been proposed by Raman *et al.* (2009) in the field of abdominal laparoscopy. Their research eliminates the need for multiple incisions during a laparoscopy and instead, a single incision is made through which all the necessary equipment is inserted into the abdomen. The internal surgery tools are then attached to

the magnetic anchoring and guidance system (MAGS) ports that are located in various positions on the skin's surface. Thus the tools have to be operated wirelessly, which can be seen as an alternative to telemedicine robots.

Best and Cadeddu (2010) propose further changes to the MAGS system, for example, the ability to move the external magnets on the patient's skin and thus be able to operate the internal tools. They further comment on the disadvantage of said system, which is the use of permanent Neodymium-Iron-Boron, NdFeBr, magnets. The authors note that prolonged use could lead to bruising of the tissue as a result of the clamping action between the external and the internal magnet. A further downside is that the magnets cannot be switched off which could lead to complication when trying to remove the two magnets from one another.

Lastly, Kume *et al.* (2008) describe the use of permanent magnets as bowel lumen anchors during colon surgery. Their study involves a permanent magnet being inserted into the rectum which can be anchored to the abdominal wall by an external magnet. As an advantage they mention that the limited attraction force between the internal and external magnet prevents mechanical tissue damage, as too much force separates the magnets. In conclusion they add that the external anchor greatly improves laparoscopic access to the point of dissection due to the fact that less tools have to be inserted into the abdomen. Figure 2.7(a) depicts the use of permanent magnets to anchor the rectum, whereas Figure 2.7(b) depicts organ manipulation as per Kume *et al.* (2008).

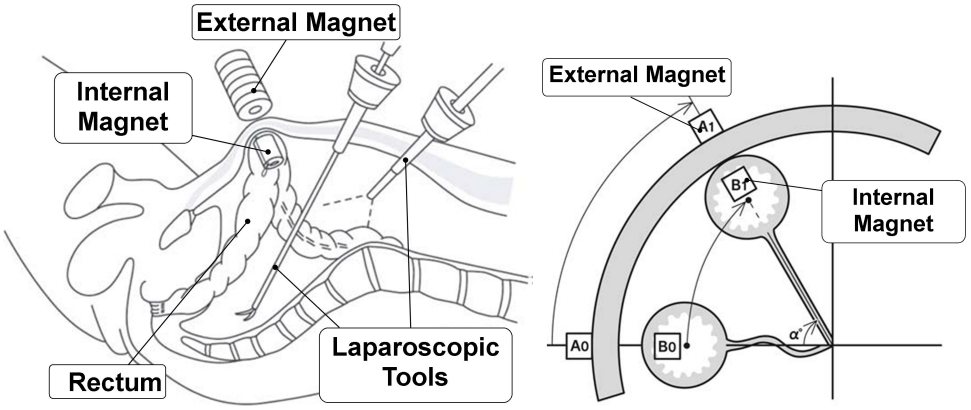

(a) Magnetic Bowel Anchor (b) Anchor Manipulation

Figure 2.7: Magnetic Bowel Anchoring and Internal Manipulation (Image adapted from Kume *et al.* (2008))

Research into magnetic manipulation of objects inside the human body has been done by numerous authors. The most noteworthy research has been in the field of magnetic stereotaxis systems for cardiac and cranial catheter manipulation. Stereotaxis means "touch in three dimensions". This system was

designed to give surgeons a sense of dimensionality when performing delicate operations like cardiac catheter manipulations. It can be combined with the field of haptics, to give real-time feedback to the surgeon as he controls the catheter via remote wireless systems. Magnetic stereotaxis involves the use of large electromagnets to manipulate the surgical tip.

Grady *et al.* (1990) discuss using a single coil to guide a catheter by rotating the coil about a central axis of the patients head. The coil current can be varied to either allow the magnetic catheter tip to rotate or to move forward slightly. The coil uses pulses of up to 500 A/mm^2 to create a magnetic gradient of between 5 - 8 Tesla. In further research Meeker *et al.* (1996) and Grady *et al.* (2000) describe an upgraded design of the magnetic stereotaxis system consisting of three pairs of superconducting coils which have to be cooled with liquid nitrogen to prevent overheating. Coolant is a necessity as coil pulse current densities reach up to 1000 A/mm^2. As an alternative to the coils moving around the patient they remain stationary and only their magnetic field is altered to create a magnetic force vector for the catheter tip. The reported accuracy of the system was sufficient to warrant further study as the catheter tip always remained within 1.5 mm of the target path.

Similar studies have been done on cardiac catheter manipulation. Faddis and Lindsay (2003) describe the use of three coil pairs, as described earlier, to orientate a magnetic catheter tip in cardiac catheter manipulation. Lastly, a study by Moore (2005) reports the use of an MRI machine to monitor the position of a catheter tip during catheterization. In accordance with this study a tiny coil is wrapped around the catheter tip which, when under the influence of the magnetic field of the MRI, has a current induced in its windings. This shows up as noise on the imaging screen, which greatly simplifies catheter location.

Another interesting application for magnets can be found in the field of endoscopy. Wang and Meng (2007) propose and test a system similar to the three coil pair stereotaxis system to manoeuvre an endoscopic capsule through the intestine. The capsules that were tested contained cylindrical permanent magnets with diameters ranging from 8 - 13 mm. The friction force in the intestine that had to be overcome, ranged from 20 mN to 150 mN with respect to the various diameters. To calculate the torque and force values on the internal magnet by the external coils, the internal magnets are treated as dipoles to simplify the problem and eliminate geometry constraints in calculations. The outer coil diameters ranged from 0.37 m to 0.5 m and the distance between coil pairs was reported to be 0.4 m. Simulation results concluded that an absolute current density of 344 A/mm^2 was necessary to impose a pulling force of 1 N on the internal capsule.

A different approach to endoscopic capsule approach was taken by Ciuti *et al.* (2010). Their system makes use of a single permanent magnet attached to a robotic arm to manoeuvre the internal magnetic capsule through the gastrointestinal tract. The proposed internal capsule weighs approximately 32 g

which translates to a pulling force of 315 mN that the external magnet has to exert on the capsule. For the external magnet they chose a cylindrical N35 NdFeBr rare-earth magnet with a residual flux density of 1.21 Tesla. Its diameter and length are 60 mm and 70 mm respectively and it was magnetized radially to be able to impose accurate pitch and yaw control on the internal magnet. To be able to accommodate the capsules cylindrical shape, four axially magnetized cylindrical N35 NdFeBr magnets are attached in a concentric pattern around the capsule as depicted in Figure 2.8(b).

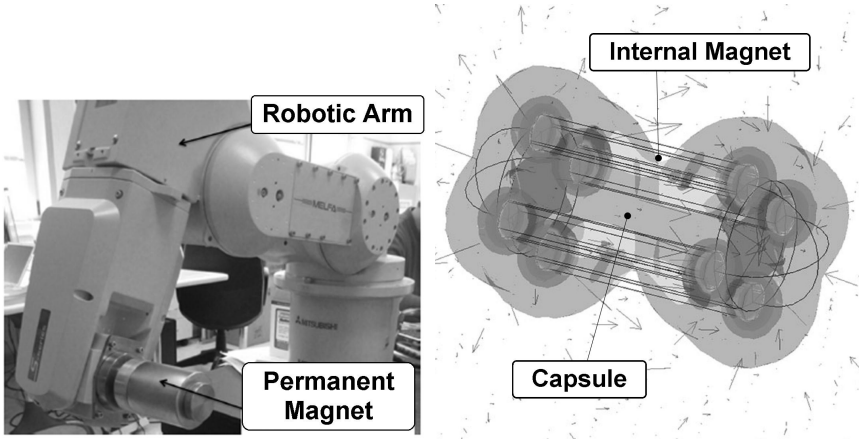

(a) Robotic Arm (b) Internal Magnet Configuration

Figure 2.8: Robotic Endoscopic Manipulation (Image adapted from Ciuti *et al.* (2010))

The system was successfully tested *ex-vivo*, displaying excellent control over the internal capsule. Further study is still necessary to determine a solution for cases where the capsule is unable to rotate, for instance in a partially collapsed lumen.

Swain *et al.* (2010) also suggested the use of magnets in endoscopy. Instead of utilizing robotic manipulation however, they opted for a simpler approach by manipulating the external magnet manually. As with Ciuti *et al.* (2010) the internal capsule is fitted with NdFeBr magnets which are then swallowed and can be manipulated via a hand held external magnet which is held close to the patient's skin surface. The research team reported excellent manipulation results, but note that as the distance between the two magnets increases, the attraction force decreases exponentially. Negative results for manipulation are thus expected with severely obese patients.

In conclusion, the research above shows that magnetic manipulation of catheters or capsules in the human body is indeed possible and definitely warrants further research. As magnetic field interaction is almost commonplace in modern surgeries, the next section deals with possible risks that are associated with the added magnetic field exposure.

2.3.2 Influence of Magnetic Fields on patients

Since magnetic flux densities breach ever higher limits with newer magnetic designs and discovery of Type 2 superconducting magnets, research into the influences of these magnetic fields on patients becomes ever more relevant. A study by Schenck (2000) reveals that almost all of the 100,000,000 MRI studies performed on patients since the dawn of MRI machines (in the 1980's) were carried out without any evidential harm by the strong static magnetic field. The few accidents that did occur were attributed to ferromagnetic materials (as found in implants) and cardiac pacemakers being present in the patients.

A number of studies were conducted in the 1950's and 1960's by Barnothy *et al.* (1956) and Klitzing (1986) to investigate the influence of up to 0.35 Tesla magnetic fields on retardation of cell growth, white blood cell counts and delays in auditory evoked potential in the brainstem. The reported results were positive but subsequent studies by Eiselein *et al.* (1961) and Buettner (1992) under higher fields of between 2 and 2.5 Tesla could not confirm the findings.

Budinger *et al.* (1981) wrote in his study that there is "no positive scientific evidence for detrimental human health effects from static magnetic fields". He further concludes that despite the vast literature on magnetic influence on humans, animals or cells, no protocol was ever established that led to similar positive results when repeated. A further noteworthy study by Berry and Geim (1997) describes a frog being levitated in a record-breaking 16 Tesla magnetic field. According to them, the frog emerged from the experiment without suffering any visible biological or physiological effects.

One of the reasons of the apparent lack of risk of high magnetic fields is the fact that most human tissue has a susceptibility, χ, $\pm 20\%$ from that of water, where $\chi_{H_2O} = -9.05 \times 10^{-6}$ in SI units (Schenck *et al.*, 1996). Magnetic susceptibility is a dimensionless constant which describes the proportional relationship between a magnetized object and the applied magnetic field. This can also be written as a scalar equation, $\mathbf{M} = \chi\mathbf{H}$, where $\mathbf{M}$ is the magnetization of the object, $\mathbf{H}$ is the magnetic field strength and both measure in Ampere per meter ($\frac{A}{m}$). Figure 2.9 depicts the range of observed magnetization values, ranging from diamagnetic to ferromagnetic materials.

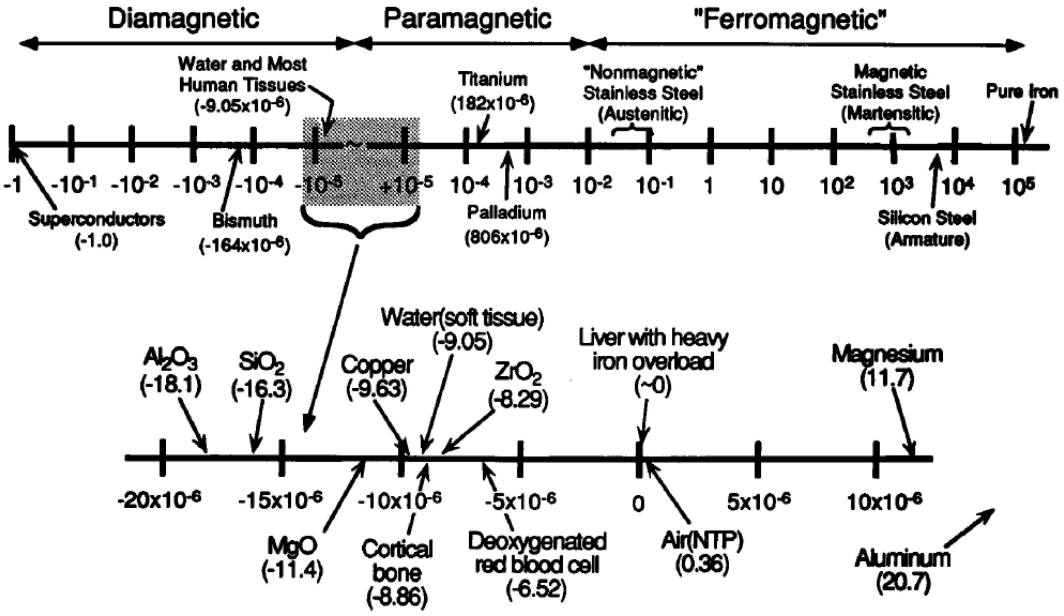

Figure 2.9: Susceptibility spectrum for known materials (Image: Schenck *et al.* (1996))

As shown above, human tissue lies at the border between diamagnetic and paramagnetic materials. This means it is only very minutely magnetized, even by strong magnetic fields, therefore eliminating any dangers of physiological tissue damage.

Within the scope of this project, influences of magnetic fields on tissue cannot be ignored. However, in light of previous research mentioned in this section, any harmful effects of magnets up to 1.3 T acting on a small body volume can be safely excluded. Since the magnetic field of the system developed in this thesis will not exceed 1.2 Tesla, will only act on a very small portion of the body and in light of the aforementioned research, it is safe to assume that this device will not have any negative impact on the health of a patient.

2.4 Essential Magnetic Theory particular to the Research

To fully describe a magnetic field it is essential to understand the basic theory behind it. Although the field of a magnet is very real and can be felt in the physical world, it is a very abstract concept. To describe this field, a vector, **B**, is used, which denotes *magnetic flux density*. This vector is displayed as curved lines on magnetic diagrams. These flux lines depict both the magnitude and the direction of the flux. Thus the logical conclusion is that the closer the flux lines are spaced to one another, the higher the flux density, ergo the term

magnetic flux density. A good analogy for **B** lines would be to compare them to rubber bands that form an elastic connection between the magnet and the attracted object, either pulling the object towards or pushing it away from the magnet. Figure 2.10 depicts two magnets with different flux densities (Rizzoni, 2007).

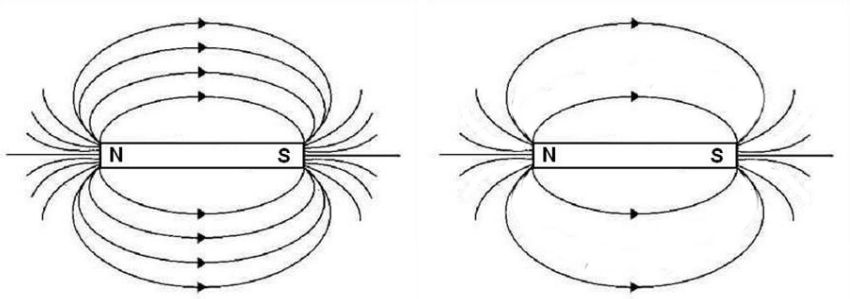

(a) High Flux Density (b) Low Flux Density

Figure 2.10: Comparison of Magnetic Flux Densities (Image adapted from Ciuti *et al.* (2010))

There is a direct correlation between the flux density and the strength of a magnet. Thus, the higher the flux density, the stronger the magnet.

In electrical magnets, current gives rise to a magnetic field. To describe the relationship of current and the resulting magnetic flux density, a new variable **H** is introduced, which has a relationship with both the current **i**, and the flux density, **B**. **H** is called the magnetic field intensity and can be related to **B** via the Equation 2.1.

$$\mathbf{H} = \mu_0 \mathbf{B} \tag{2.1}$$

where μ_0 is a dimensionless universal constant called the permeability of air and has a value of $4\pi \times 10^{-7}$. Every material has a different intrinsic μ_r value, known as the relative permeability. Consequently, to compare **B** and **H** in a material other than air, μ_r and μ_0 are combined in Equation 2.2 as follows:

$$\mathbf{H} = \mu_0 \mu_r \mathbf{B} \tag{2.2}$$

This relationship between **B** and **H** can be graphically displayed on a curve called the *B-H curve*. As seen in Figure 2.11, the curve can be described by three distinct features namely the steep initial phase, the knee and the saturation phase (Edwards, 2007). Thus, μ_r varies with changing **B** and **H** in magnetic materials. During the initial phase it is seen that the flux density of the material increases greatly with little increase of the field intensity, **H**.

After the knee phase though, the material becomes saturated with magnetic flux and an increase in **B** is only possible with greater increase in **H**.

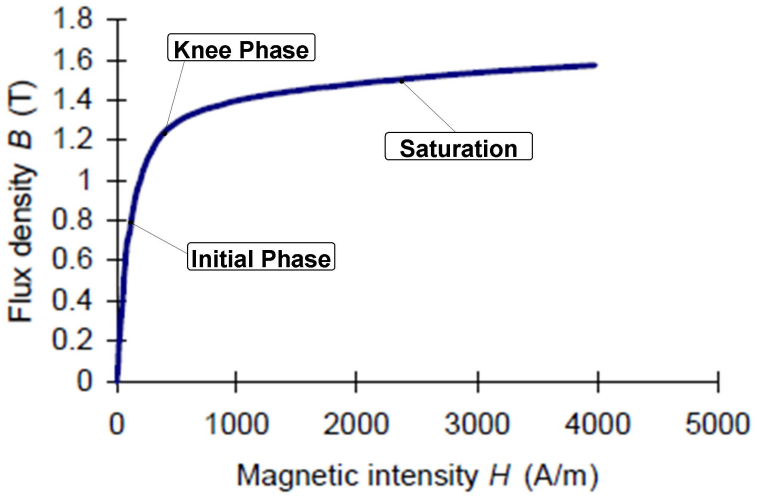

Figure 2.11: B-H curve of soft steel
(Image: IMTRONICS Institute, Thessaly, Greece)

The last piece of relevant theory deals with permanent magnetism. For some materials a certain magnetization remains after the electric field is removed. Figure 2.12 depicts this characteristic, from which it is also clear that for permanent magnetic materials the important section of the B-H curve lies in the second quadrant. After the applied external field is removed, the magnetization of the material does not decrease back to zero, but instead, crosses the **B**-axis from whereon it attains a negative field intensity value. The value of **B** when the applied field intensity **H** is zero is called the remnant flux density, B_r. H_c on the graph can be described as the negative value of **H** that must be applied to the permanent magnet to reduce **B** back to zero and remove the magnetization (Rizzoni, 2007).

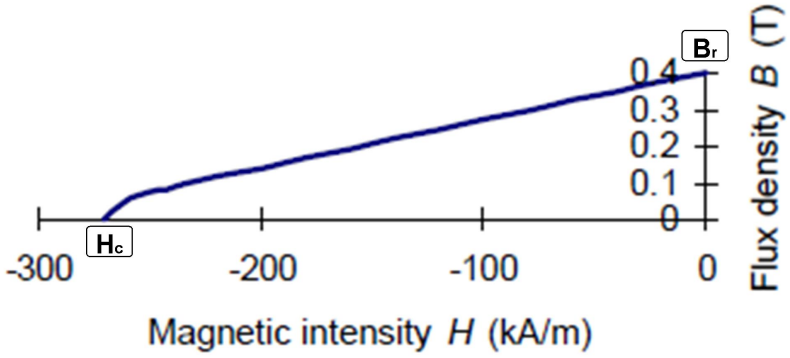

Figure 2.12: Demagnetization curve of ceramic ferrite (Image: IMTRONICS Institute, Thessaly, Greece)

In conclusion, the theoretical material discussed in this section is essential to differentiate between different types of magnets and how they operate. Electromagnets operate on quite different principles compared to permanent magnets and this needs to be taken into account in the design of the external magnetic manipulator.

2.5 FEA - Finite Element Analysis

In layman's terms, Finite Element Analysis (FEA) is a method that takes a given structure, cuts it up into a desired number of pieces (elements), describes the behaviour of each little piece in an elementary way and then reconnects these pieces at points called "nodes". The result of this is a large number of simultaneous equations (depending on the number of elements) which can be solved algebraically. As there may be quite a large number of these equations, computers are implemented to solve the problem (Cook, 1995). A more complex explanation describes the finite element method as a piecewise polynomial interpolation. This means that over a field , or mesh, a quantity such as displacement or stress is interpolated from surrounding nodes. Thus by making the element size ever smaller, interpolations between nodes become more accurate. In order to increase accuracy over the mesh, field quantities at nodes are sought that minimize certain functions, for example, total energy. Through this minimisation process simultaneous algebraic equations are created for the field quantities at nodes. To denote this we use the matrix equation $\mathbf{KD} = \mathbf{R}$, where $\mathbf{K}$ is a matrix of known constants, $\mathbf{D}$ is a vector of unknowns and $\mathbf{R}$ is a vector of known loads. A classical example of $\mathbf{K}$ would be in stress analysis, where it is known as the "stiffness matrix" (Cook, 1995). Figure 2.13 depicts a FE analysis of stresses on a human foot.

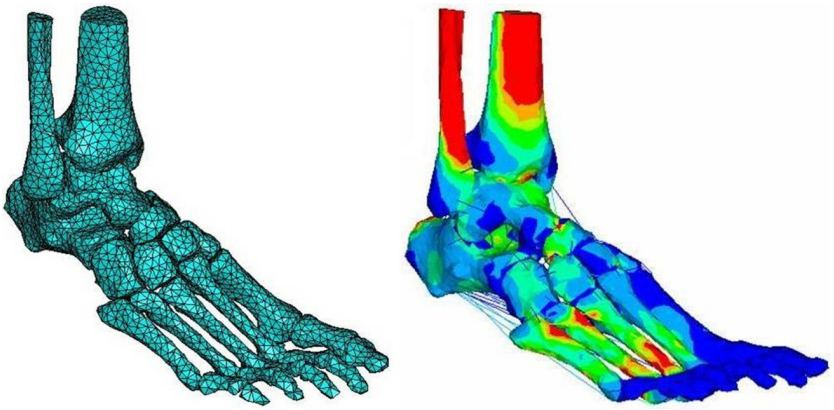

Figure 2.13: FE Analysis Example of stresses on a human foot (Image: IMTRONICS Institute, Thessaly, Greece)

As can be seen in the image on the left, during post-processing, the foot model is set up and is divided into numerous minute triangular elements. After the computer solves the model, foot stresses can be displayed in a post-processor as depicted in the image on the right. In this case the stresses are depicted in colour according to stress gradients, where red depicts the highest stresses and blue the the lowest.

It is generally good practice to be critical of an FEA solution as it is easy to misinterpret a solution if, for instance, the mesh size was set up incorrectly. Cook (1995) states that if using FE analysis the user must understand how the program analyses nodes and elements in order to successfully utilize its computational power. Thus, a good physical understanding of the problem is necessary to be able to detect errors and understand results. Lastly, it is essential for the FEA model to be verified experimentally in order to gauge the accuracy and performance of the model. FEA models should be continually improved to minimize the error between the simulation and the experimental results and to increase the confidence in the simulation results.

2.5.1 FEA as a tool to solve Magnetic Circuits

Today, FEA is available for almost any engineering problem, including heat transfer, fluid flow and the analysis of magnetic fields. This section will deal with the advances of FEA as a tool for magnetic field analysis. Throughout this thesis, Infolytica's MagNET v6.7 will be used to model different magnetic elements to test certain designs. It is therefore important to understand the principles on which the software is based as it iterates towards a solution. A static magnetic field can be described by a set of equations from Maxwell's classical electrodynamic foundation. These equations are:

$$\nabla \times \mathbf{H} = \mathbf{J} \tag{2.3}$$

$$\nabla \cdot \mathbf{B} = 0 \tag{2.4}$$

$$\mathbf{B} = \mu\mathbf{H} = \mu_0\mu_r\mathbf{H} \tag{2.5}$$

where Equation 2.3 is called the differential Ampere's Circuital law, which relates magnetic fields to electric currents that produce them. Equation 2.4 is called Gauss's Law for Magnetism, which basically describes that free magnetic monopoles cannot exist, and Equation 2.5 describes the relationship between $\mathbf{B}$ and $\mathbf{H}$. In the above equations $\mathbf{J}$ is called the current density and μ_0 and μ_r are the permeability of air and the relative permeability of a substance respectively (Edwards, 2007). Since Equation 2.4 = 0, there exists a vector potential $\mathbf{A}$ such that:

$$\mathbf{B} = \nabla \times \mathbf{A} \tag{2.6}$$

It is rather difficult to visualize, but the simplest way to describe $\mathbf{A}$ would be to view it as a field of curling rings around a ring of $\mathbf{B}$ in a toroidal conductor. Equation 2.6 can be combined with Equation 2.3 and Equation 2.5 to form

$$\nabla \times (\frac{1}{\mu}\nabla \times \mathbf{A}) = \mathbf{J} \tag{2.7}$$

This last equation can be solved numerically with the help of finite element analysis to calculate the magnetic field in a simulation. Thus, for a non-linear magnetic material the solver starts by choosing μ from the initial slope of the specific B-H curve for that material. From this initial point the solver solves for the magnet vector potential, $\mathbf{A}$, and the current density $\mathbf{J}$, using the conjugate gradient method. Once a solution is reached the flux density, $\mathbf{B}$, can be calculated. Finally this $\mathbf{B}$ can be related back to the B-H curve to acquire a new value for μ. Iteration of this process continues until the μ values converge, or a certain required accuracy tolerance is reached. Once the flux density $\mathbf{B}$ is found, all the other vector fields can be found by using Maxwell's remaining equations (Edwards, 2007).

This concludes the literature study. Chapter 3 will focus on making use of the literature study to develope concepts for the manipulator design.

Chapter 3

Conceptual Design

Uterine manipulators are very helpful tools in laparoscopic surgeries. Unfortunately, as helpful as they may be, existing manipulators do pose a number of disadvantages. As summed up in Table 2.1, Section 2.2.3 most manipulators are very expensive. This expense is firstly due to manufacturing cost, secondly because the surgeon requires extra assistance in the theatre to handle the manipulator and thirdly because many manipulators are non reusable. Most uterine manipulators are also complex to assemble and require training to operate. Lastly, but most importantly, existing manipulators can cause tissue trauma and surgical bleeding which in turn causes discomfort to the patient and can increase recovery time.

The aim of this chapter is to take the advantages and disadvantages of existing manipulators into account and design a device, utilizing magnets, that incorporates the strengths and eliminates the weaknesses of current tools. Figure 3.1 describes the overall concept of a magnetic manipulator.

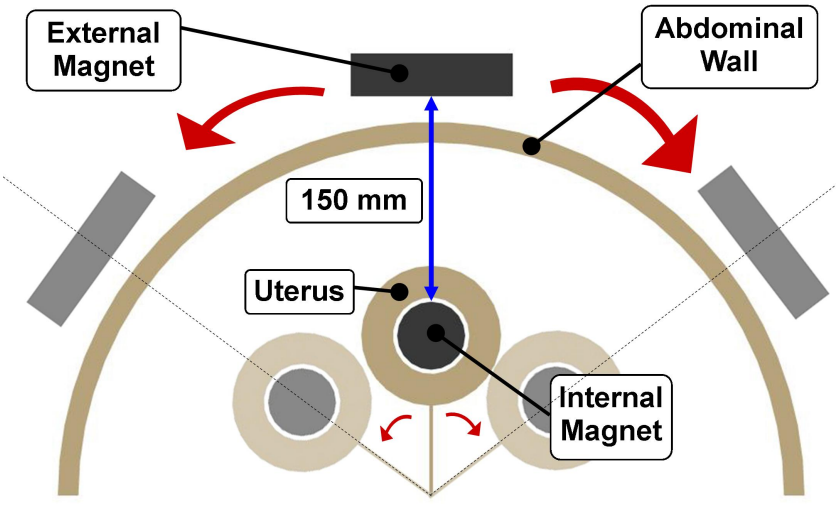

Figure 3.1: Brief Description of the Concept

As depicted, the magnetic attractive force has to breach an air-gap of roughly 150 mm. Furthermore, as the external magnet is manipulated on the outside of the patient's body, the internal magnet is forced to move with it due to the magnetic attraction force. This outlines the basic concept of magnetic uterine manipulation. This chapter is divided up into sections outlining the conceptual design of the different substructures of the entire manipulator which include the external magnet, the internal magnet and the actuating platform.

3.1 External Magnet Concept Evaluation

Strong emphasis was placed on selecting the proper magnets for the device. There are a number of different types of magnets and magnet configurations to consider. Research was done on magnet shapes, different types of permanent magnets, electromagnets, permanent-electromagnet hybrids and even different magnet housing configurations. The requirement for these magnets was to be able to lift a load of at least 1 N over a distance of 150 mm. The load requirement of 1 N was derived from the average weight of a uterus of 80 g (0.785 N) as per Martini *et al.* (2000). The air-gap of 150 mm was derived from the minimum distance possible between the external and the internal magnet. This air-gap takes the distance between the patient's uterus and the external abdominal surface, as well as the the minimum distance of the external magnet from the patient's abdominal surface of 20 mm into consideration Ciuti *et al.* (2010). Furthermore, for the purpose of this thesis, the magnetic influence of human tissue was assumed to be the same as that of air, as per Figure 2.9, to simplify modelling. Consequently, the gap between the two magnets was modelled as an air space.

3.1.1 Electromagnets

Electromagnets work on the principle of a current conducting wire tightly wrapped around a magnetically permeable core, which induces an electromagnetic flux (emf) in the core. The core absorbs the flux, essentially compressing it, and acts as an amplifier to expel the field further away from the poles. The strength or flux density, B, of the electromagnet is directly influenced by the number of turns, N, the current running through the wire, i, and the length of the core, l, according to Equation 3.1 (Rizzoni, 2007).

$$B = \frac{Ni}{l} \tag{3.1}$$

Another factor that influences the flux density is the diameter of the core material, as the more core material there is, the higher the degree of permeability which considerably increases magnetic flux density in the coil. Elec-

tromagnets come in different shapes and can be designed with different core materials. Figure 3.2 displays two different electromagnet configurations.

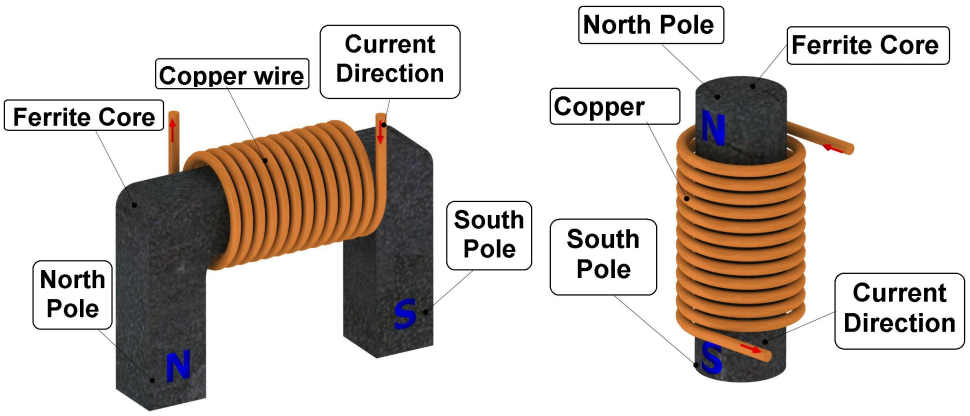

(a) Horseshoe Magnet (b) Cylindrical Magnet

Figure 3.2: Types of Electromagnets

As can be seen, their layout is similar but the configuration of the poles differs. All magnets have this basic layout as they all function on the same principle of flux flowing between two poles with different polarity. The distance between poles and their orientation can be changed to alter the field and tailor the magnet to certain needs.

Electromagnets have the advantage of being switchable when the need arises. This means their polarity can be altered by changing the direction of the current or they can be turned off all together. Furthermore, the field strength of the magnet can be directly controlled by altering the coil supply current. This means that the distance between the electromagnet and the object it attracts can be kept constant by means of a control system. A similar system is employed in magnetic levitation (MagLev) of high speed trains (Xu *et al.*, 2004).

The disadvantages of electromagnets are that they require a very high supply current or a substantial number of windings to be able to produce high enough flux density to bridge a large air gap. The duty cycle of an electromagnet depends on the amount of current pushed through the coil. This means that the coil might overheat if the duty cycle is too high and a means of cooling, like oil or water cooling, has to be introduced. Something that should also be taken into account is the remanant flux in the ferromagnetic core after the magnet is shut down. This means the core is still slightly magnetized after the external magnetic field has been removed, which can be a hazard.

3.1.2 Permanent Magnets

Permanent magnets have exactly the same magnetic properties and pole configurations as electromagnets. The only difference is that permanent magnets can retain their field without an external field excitation. Modern magnetic materials have a very high coercivity, which means they have a high resistance to becoming demagnetized or having their magnetic field reversed. This property is important when working with two opposing permanent magnets with a small air gap between them as it keeps either magnet from being demagnetized by the other's magnetic field. The material used can be magnetized in a manner of different ways, and orientations, resulting in a variety of magnet shapes tailored to specific applications. Figure 3.3 depicts typical magnetization directions of certain magnets in relation to their geometry.

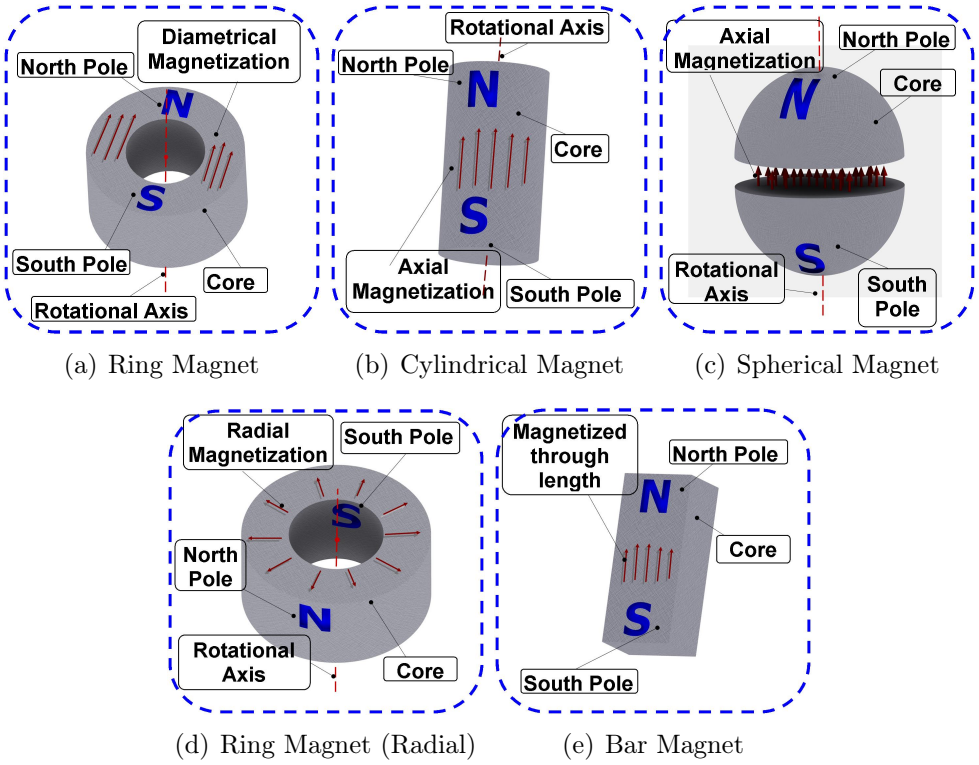

(a) Ring Magnet (b) Cylindrical Magnet (c) Spherical Magnet

(d) Ring Magnet (Radial) (e) Bar Magnet

Figure 3.3: Permanent Magnet Magnetization Direction

There are also a number of different ways to manufacture these magnets to specification. Methods include sintering, casting, bonding and moulding. The material is magnetized during, or after, manufacturing with the help of strong electromagnets that work by aligning the internal domains of the material.

An advantage of permanent magnets is their high field strength to volume ratio. This ratio is much higher than that of their electric counterparts. A rare earth Neodymium magnet can have a remanent flux density of up to 1.4

Tesla, whereas an electromagnet would need a high current and a considerable number of windings to achieve a similar flux density. Furthermore, permanent magnets are not dependant on a current for their field strength, therefore no cumbersome power source is needed. Permanent magnets thus offer a low power solution for large air gap problems.

The disadvantage of these magnets is that they cannot be turned off. They have a very high contact force which means that if they come into contact with a magnetically permeable material it is difficult to remove them and it could become hazardous if human tissue was clamped between these surfaces.

3.1.3 Hybrid Magnet Configurations

Hybrid magnet configurations, or electropermanent magnets, are, as the name suggests, a combination of electromagnets and permanent magnets. Shirazee and Basak (1995) suggest in their work that hybrid magnets overcome the large air gap shortcomings of electromagnets by combining them with permanent magnets. The bulk of the work of the hybrid is done by the permanent magnet, whereas the function of the electromagnet is to enable position control of the attracted magnet. Figure 3.4 depicts a hybrid magnet assembly.

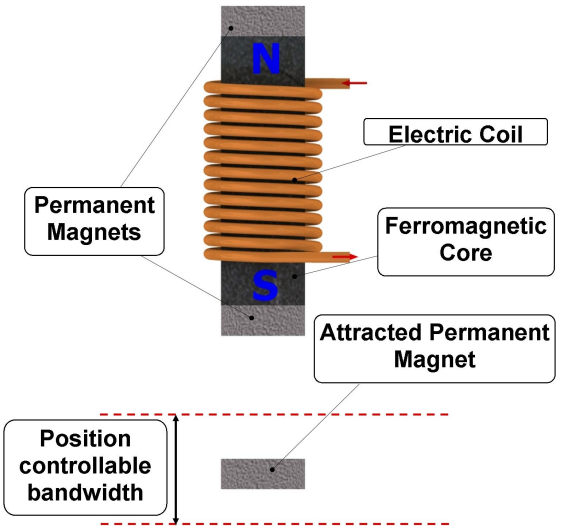

Figure 3.4: Hybrid Magnet Assembly

Position control of the attracted permanent magnet is unfortunately only possible within a certain bandwidth. As explained earlier, position control is achieved by alternating the electromagnetic field to counteract or add to the field of the permanent magnets at the poles. This increases or decreases the depth of magnetic field penetration which controls the magnitude of the attraction force on the attracted magnet.

An advantage of these magnetic assemblies is the fact that they have a partially controllable magnetic field that only requires a fraction of the current of a normal electromagnet to produce the same deep magnetic field pattern. This also means that the magnet is smaller in dimension than its electric counterpart. Thus it can be summed up that electropermanent magnets can lift significant weights over increasingly large air gaps (Shirazee and Basak, 1995).

Disadvantages of electropermanent magnets are that they can only control the flux density at a certain bandwidth distance away from the assembly, as depicted in Figure 3.4. Once the external magnet breaches the bandwidth boundaries, it is either attracted by the electropermanent magnet or it falls out of suspension. A further disadvantage is that the electropermanent magnet requires a power source to function.

3.1.4 Permanent Magnets with Shielding

Magnetic shielding warrants a concept design as it could be of a huge benefit in keeping the flux lines of the external magnet from being dispersed out from the top pole of the magnet and possibly causing havoc with sensitive equipment or tools. Magnetic shielding is used to guide magnetic flux lines from one pole of the magnet via a conduit (shield) and focus them around the other pole. This is depicted in Figure 3.5. If proven to work this concept would increase the safety and efficiency of any type of magnet in a surgical environment. Very little research has been done on shielding to focus magnetic flux lines, as most papers on this field focus on the actual shielding as a protection for sensitive electronic equipment from external magnetic sources. Shirazee and Basak (1995) describe the use of shields to focus flux lines with minor success at increasing deep field penetration. Thus, simulations of different shielding material and shield geometries could prove invaluable towards the development of a magnetic manipulator. Figure 3.5 depicts a permanent magnet surrounded by a conical shield to focus flux lines and prevent flux leakage from the top of the magnet.

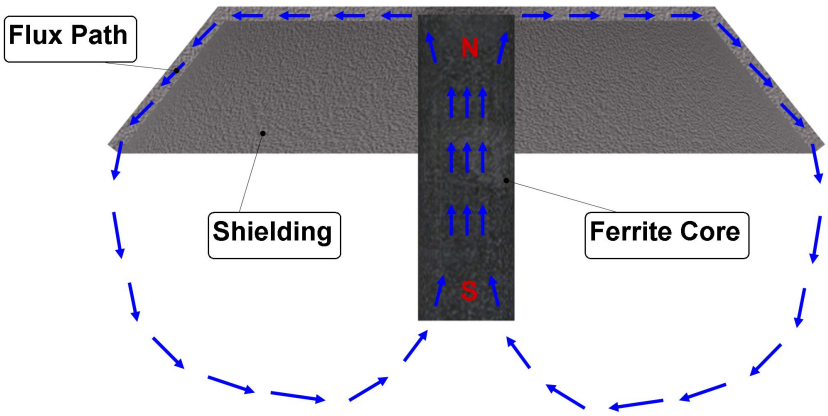

Figure 3.5: Magnet with Shielding

3.1.5 Comparison

To conclude the external magnet concept evaluation, the concepts were compared according to certain characteristics which were important in the selection of the external magnet. Although all magnets showed various advantages of other concepts, the electromagnet concept could be excluded from the study due to negative results in the literature study. Wang and Meng (2007) describe coil current densities as high as 344 A/mm^2 to create an attraction force of 150 mN over a distance of 150 mm, which would be very impractical for the purpose of this thesis. Hybrid magnets were also excluded as a final concept, as these type of magnets exhibit the same disadvantages as pure electromagnets and offer a weaker attractive force than pure permanent magnets. Table 3.1 displays factors that were considered in making a concept choice. The permanent magnet was deemed the most likely concept of fulfilling the requirements of the study, especially in the prototype design, as it required no external power source and had a very high field strength to size ratio. Magnetic shielding will also be included in the final design stage as this configuration promises an improvement of the permanent magnet's large air-gap penetrating ability.

Table 3.1: Comparison of External Magnet Concepts

Concept	High Field Strength to size ratio	Switchable	Requires Electricity	Requires cooling	Ease of Design
Electromagnet	✓	✓✓✓	✓✓	✓✓	✓✓
Permanent Magnet	✓✓✓	✗	✗	✗	✓✓✓
Hybrid Magnet	✓✓	✓✓	✓	✓	✓
Permanent magnet with shielding	✓✓✓	✗	✗	✗	✓✓

✗ = "Not Applicable", ✓= "Moderately Applicable", ✓✓= "Applicable",✓✓✓= "Very Applicable"

3.2 Internal Magnet Concept Evaluation

This section deals with the concept design of the internal magnet. The internal magnet is inserted into the uterus at the beginning of the surgery and remains there for the remainder of the procedure. As the external magnet is manipulated on the outside of the patient's body, the magnetic attraction force causes the internal magnet to move toward the external magnet thus displacing the uterus. All the magnets in the concept design were required to have housings as to forego the risk of potentially toxic corrosion of the magnets in the uterus.

3.2.1 Cylindrical Magnet in Housing

As the name suggests, this concept comprises a cylindrical magnet in a protective plastic housing. The concept was inspired by cylindrical capsules normally used in endoscopy. Figure 3.6 depicts the design of the cylindrical magnet and housing.

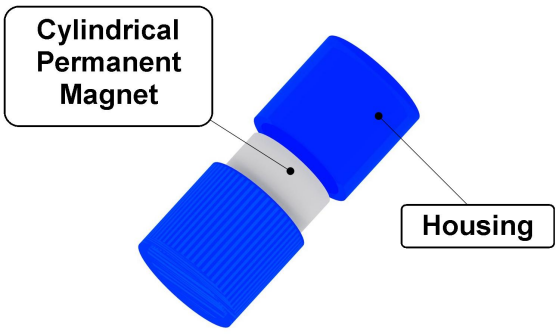

Figure 3.6: Cylindrical Magnet in Housing

An advantage of this concept is that it is easily insertable through the cervix due to its cylindrical shape.

On the down side, the magnet is not able to align to the magnetic field as it is lodged in the uterus in a permanent position. This means that the internal magnet has the potential to be repelled by the external magnet if the same poles are aligned.

3.2.2 Quad configuration of Cylindrical Magnets

Ciuti *et al.* (2010) describe the use of a capsule, around which four cylindrical magnets are aligned in a quadratic pattern, for use in endoscopy. The internal housing can be fitted with any type of sensors which might be necessary during surgery. What is not visible in Figure 3.7 is that the cylindrical magnets are also encased in a housing.

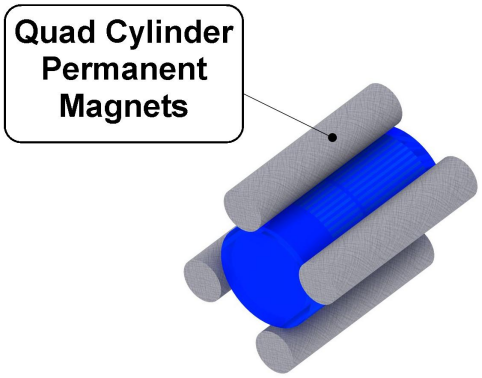

Figure 3.7: Quad configuration of Cylindrical Magnets

This concept has the advantage of being able to house any type of sensor that might be useful during surgery. In addition, its cylindrical shape makes it easily insertable albeit being somewhat bulkier than the previous concept. The disadvantage of this concept once again is the fact that it cannot align itself to an external field.

3.2.3 Miniature Electromagnet

The miniature electromagnet concept comprises a small coil wrapped around a ferromagnetic cylinder. The device is also fitted into a housing to keep the core and coil from corroding. The idea behind the electromagnet was to be able to help with position control of the cylinder. Thus the current can be altered to change the strength of the magnetic field.

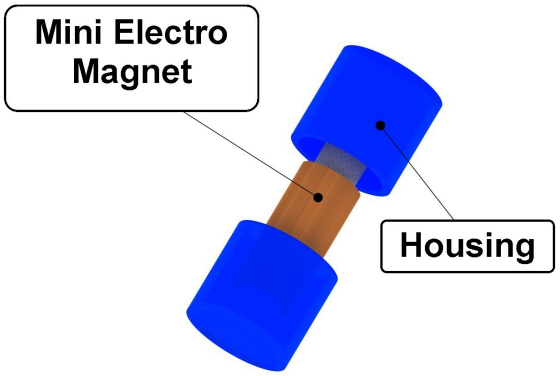

Figure 3.8: Miniature Electromagnet

The advantage of this concept is the fact that its magnetic field is switchable. This implies that although it cannot align itself to the external field, it can change its field polarity to perhaps be aligned more favourably. Furthermore, the field can be controlled, strengthening or weakening it on demand. Lastly. its cylindrical shape also makes it suitable for easy insertion into the uterus.

Disadvantages are that the device needs a current source to power the magnet. This means that either batteries need to be added to the capsule, or a wire needs to be attached from the internal magnet through the cervix to an outside power source. Moreover, the magnetic field might not be as strong as that of a permanent rare-earth magnet.

3.2.4 Spherical Magnet in Housing

Instead of using a cylindrical magnet in a housing, this design utilized a spherical magnet which is magnetized diametrically. The housing of the magnet has to be moulded properly and treated to a smooth surface finish to allow for rotation of the sphere.

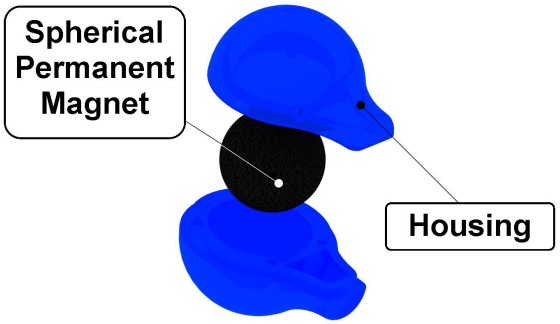

Figure 3.9: Spherical Magnet in Housing

The advantage of this design is the fact that the spherical magnet is able to align itself to an external field, thus always presenting the strongest attraction force possible. The spherical design is also more ergonomical which should make it easy to position tightly in the uterus. A disadvantage of this design is that, diametrically it might be a bit larger than the cylindrical designs, thus making it more difficult to insert.

3.2.5 Comparison

Table 3.2 summarizes the strengths and weakness of the individual internal magnet concepts. It is clear from the comparison that the spherical magnet

design has properties which are very desirable for an internal magnet. The fact that it is self aligning to the external magnetic field makes it the obvious concept choice, as an aligned inner magnet will always present the strongest attraction force between both magnets.

Table 3.2: Comparison of Internal Magnet Concepts

Concept	High Field Strength to size ratio	Self Aligning	Ease of Insertion	Requires Power source
Cylindrical Permanent Magnet	✓✓✓	✗	✓✓	✗
Quad Cylindrical Permanent Magnets	✓✓	✗	✓✓	✗
Mini Electromagnet	✓	✓	✓✓	✓✓✓
Spherical Permanent Magnet	✓✓✓	✓✓✓	✓	✗

✗ = "Not Applicable", ✓= "Moderately Applicable", ✓✓= "Applicable",✓✓✓= "Very Applicable"

3.3 Actuator Concept Evaluation

This section deals with the concept evaluation of the actuator responsible for manipulating the external magnet. Most of the concepts have an arch as a common design feature, as it proves to be an effective platform to manoeuvre an external magnet around a patient without obstruction.

3.3.1 Magnetic Array Setup

The magnetic array concept was inspired by the design and function of a stepper motor. Figure 3.10 depicts the layout and a functioning diagram of the concept.

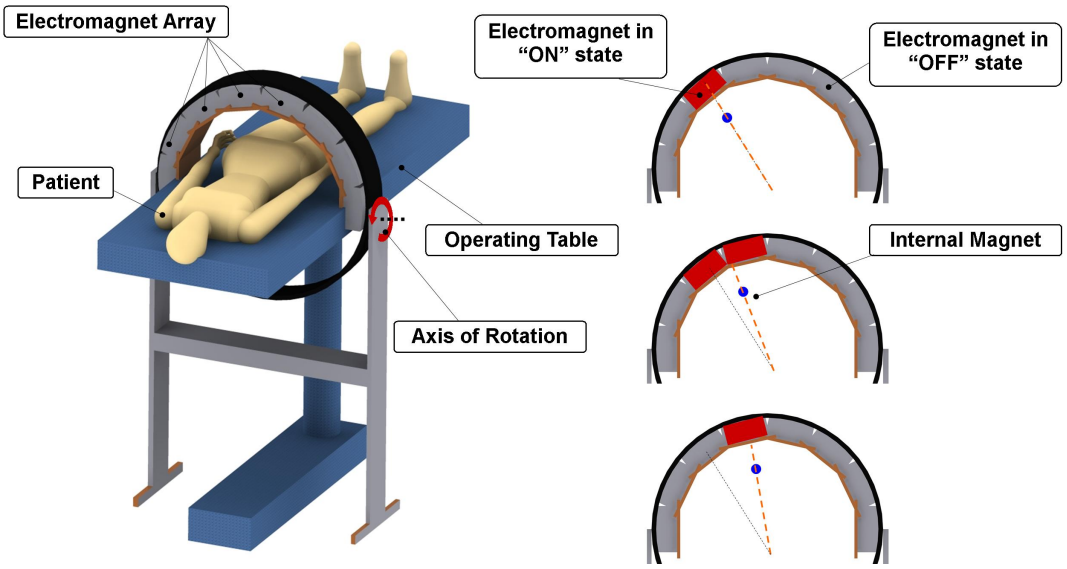

Figure 3.10: Magnet Array Setup and Functional Diagram

As explained in the previous diagram, an electromagnet array is arranged in an arch around the patient. The arch is able to rotate on an axis perpendicular to the sagittal (median) plane of the patient. To rotate the internal magnet on an axis perpendicular to the transverse plane, the electromagnets on the arch are switched on in succession. As in a stepper motor, once the first magnet is switched on, the internal magnet is suspended in its field. When the adjacent electromagnet is switched on, the magnetic field of the two electromagnets combine and a magnetic focus point is created between them, thus pulling the internal magnet towards this point. The next step involves the first electromagnet switching off so that the magnetic field is created solely by the second electromagnet. In so doing, the internal magnet is pulled towards the second electromagnet. This process is repeated over the whole array of electromagnets and can also be reversed. The process is depicted in detail in the functional diagram in Figure 3.10.

An advantage of this setup is the lack of moving parts to manipulate the internal magnet. The only part that needs to be rotated is the arch itself. Furthermore, the position of the internal magnet can be accurately controlled by gradually varying adjacent electromagnet field strengths.

Unfortunately this setup requires the use of electromagnets as permanent magnets are not able to vary their field strength. This means the electromagnets would have to be considerably large in diameter, have a large number of windings and carry a high current to be able to bridge the large air gap. A further disadvantage is that as the number of high current devices increases, so does the risk of using the device. This especially applies to a hospital environment where it is paramount to minimize the potential risk to a patient.

3.3.2 Stereo Magnet Setup

The stereo electromagnet concept was inspired by magnetic stereotaxis systems. In this case only a single coil pair would be utilized. The ring setup to which the magnets are attached is able to rotate around an axis perpendicular to the transverse as well as axis perpendicular to the sagittal plane. To manipulate the internal magnet the two opposing coils would compliment each other keeping the internal magnet suspended in their field. Thus, to move the uterus in the anterior direction, current flow to the top electromagnet is increased, whereas the bottom electromagnet current is decreased or even reversed.

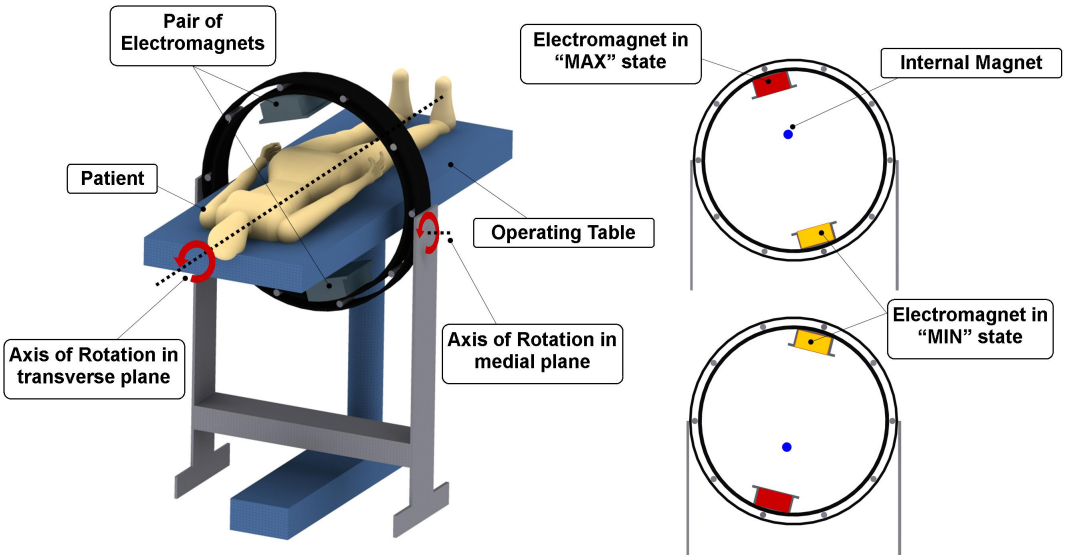

Figure 3.11: Stereo Magnet Setup and Functional Diagram

Advantages of this setup are that the strength of the magnets can be controlled and the arch can be easily operated via two motors which makes operation very smooth.

Disadvantages are that the theatre table will have to be made of a material which is permeable by magnetic flux for the bottom magnet to be of any use. Lastly, a large power source will have to be supplied to drive both electromagnets.

3.3.3 Articulated Arm

The articulated arm is a very simple design. The arm is an assembly of three or more sections with rotary joints connecting them. The base is able to rotate in the horizontal plane as depicted in Figure 3.12 and the external magnet is attached to the end of the arm. To manipulate the internal magnet, the surgeon has to manually manouevre the external magnet to the desired location. The arm is stiff enough to hold its position and anchor the internal magnet.

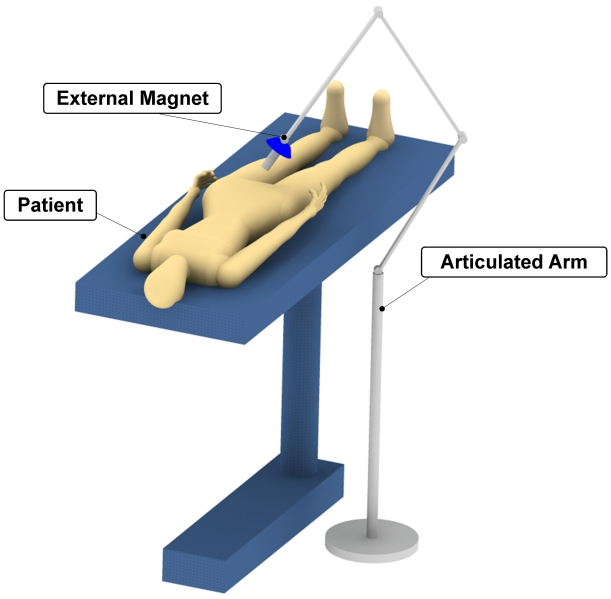

Figure 3.12: Articulated Arm Setup

An advantage of the articulated arm setup is the fact that it is a very low-tech solution. No motors or electrical controller equipment are required to manipulate the external magnet. Furthermore, the device would not need any training to operate.

Disadvantages would be, that since the arm is manoeuvrable by hand its position can easily be distorted by bumping into the device during surgery, causing risk to patients. Furthermore, manual control takes the focus off the operation, as the doctor has to release the surgical tools to manipulate the arm.

3.3.4 Cart on Arch

The final concept that was developed was a cart on arch system. This design utilizes an arch design similar to the concepts in Section 3.3.1 and 3.3.2. The cart can roll over the arch with the help of bearings and can be drawn to any position on the arch via a belt and pulley system. Figure 3.13 depicts this setup and a functional diagram thereof.

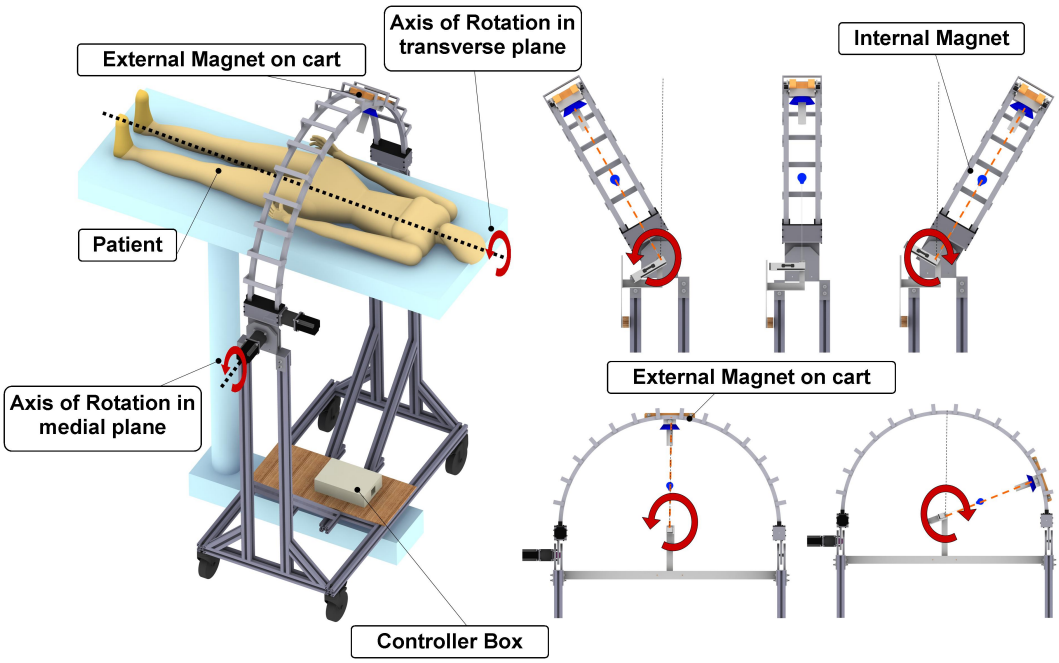

Figure 3.13: Cart on Arch Setup and Functional Diagram

As depicted, the arch itself is able to rotate on an axis perpendicular to the sagittal plane of the patient. The cart with attached magnet rotates about an axis perpendicular to the transverse plane of the patient. Thus, the axis of the external magnet will always remain perpendicular to a point within the patient's body that is estimated to be the position of the uterus, as seen in Figure 3.13. To manipulate the internal magnet, any kind of magnet discussed in Section 3.1 can be attached to the cart.

Advantages of this system include that either electro- or permanent magnets can be used. In addition, no expensive electromagnetic array has to be installed. Another advantage would be that the system is lighter due to the fact that only half an arch is utilized. This means less powerful motors are necessary, which decreases the cost.

Disadvantages of this system are that in the case of a permanent external magnet it is difficult to alter the distance between the internal and external magnet, as the magnetic strength cannot be increased. In this case an extra linear actuator will have to be installed to vary the distance between the external magnet and the patient's abdominal wall surface.

3.3.5 Comparison

Table 3.3 is a summary of the actuator concept design section. The cart on arch system sticks out as the most desirable concept, due to the fact that it does not need huge power sources to run arrays of electromagnets. Furthermore, it has

the potential to be operated by a single surgeon and its location can be fixed once positioned. In addition, its ability to accommodate either permanent or electromagnets makes it very modular. Furthermore, the articulated arm offers very good movement range. Unfortunately the solution still requires the surgeon to manipulate the arm manually. In conclusion, it was decided that the cart system would be the best suited concept for manipulation.

Table 3.3: Comparison of Actuator Concepts

Concept	External Magnet Type		Motion			Requires Electricity	Requires Assistance
	Permanent	Electro	Anteversion / Retroversion	Lateral	Elevation		
Magnet Array	✗	✓	✓✓	✓	✓✓	✓✓✓	✓
Stereo Magnet	✗	✓	✓✓	✓	✓	✓✓	✓
Articulated Arm	✓	✓	✓✓	✓✓	✓	✓*	✗
Cart on Arch	✓	✓	✓✓	✓✓	✓	✓*	✗

✗ = "Not Applicable", ✓= "Moderately Applicable", ✓✓= "Applicable",✓✓✓= "Very Applicable"
*only if the external magnet is chosen to be an electromagnet

This concludes the conceptual design. Chapter 4 will focus on taking the conceptual design and refining the concept by applying engineering principles.

Chapter 4

Design and Modelling

This chapter comprises of the design and modelling of the various components of the magnetic manipulator.

4.1 Internal Permanent Magnet

The design of the Internal Permanent Magnet (IPM) was drastically limited by the space available in the uterus. A study by Merz *et al.* (1996) concluded that the average length and width of the uterus for pre- and post-menopausal women was 7.5 cm and 4.1 cm respectively. Ellis and Mahadevan (2010) and Martini *et al.* (2000) confirm the outcome of this study. As with most uterine manipulators, the cervix will have to be dilated to enable insertion (Mettler and Nikam, 2006). The author was also present at three hysterectomy procedures, performed by Dr. G. Du Toit, to personally gain an insight into the layout and space limitations involved in such a procedure. As such, an educated decision could be made on the design of the magnet and housing. Unfortunately, the IPM could not be simulated independently from the External Permanent Magnet (EPM), as the FEA software, MagNET, outputs the force solution as a force balance between the two magnets. Consequently the EPM and IPM were modelled as one system, which will be discussed in Section 4.2.1.

As Figure 4.1 suggests, the magnet will be encased by a plastic housing. This design offers protection from the potential hazard of the magnet corroding in the uterus causing infection or irritation. It also enables the spherical magnet to rotate freely in the housing, maintaining perfect alignment with the external magnetic field and allowing for maximum attraction force between the two magnets. Furthermore, as the magnet housing, positioned in the uterus, is not able to rotate, the device eliminates the risk of tissue trauma.

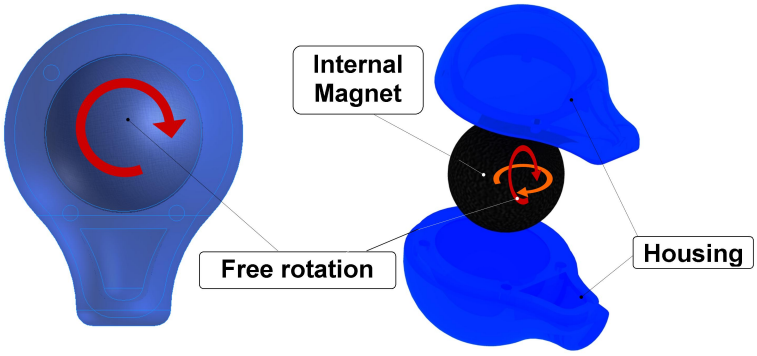

Figure 4.1: Internal Permanent Magnet Housing and Magnet Orientations

The housing was ergonomically designed with smooth edges for easy insertion and can be manufactured from bio-compatible material to prevent irritation and eliminate possible allergic reaction to the material. A spherical N38 grade NdFeBr magnet was chosen. As depicted in Table B.1 in Appendix B, these magnet types exhibit the highest flux densities of rare-earth permanent magnets and are thus the best suited magnet types for this application. Because of the availability of space in the uterus we could therefore safely choose the maximum size spherical magnet available, which had a diameter of 20 mm. Figure 4.2 depicts the position of the IPM inside the uterus.

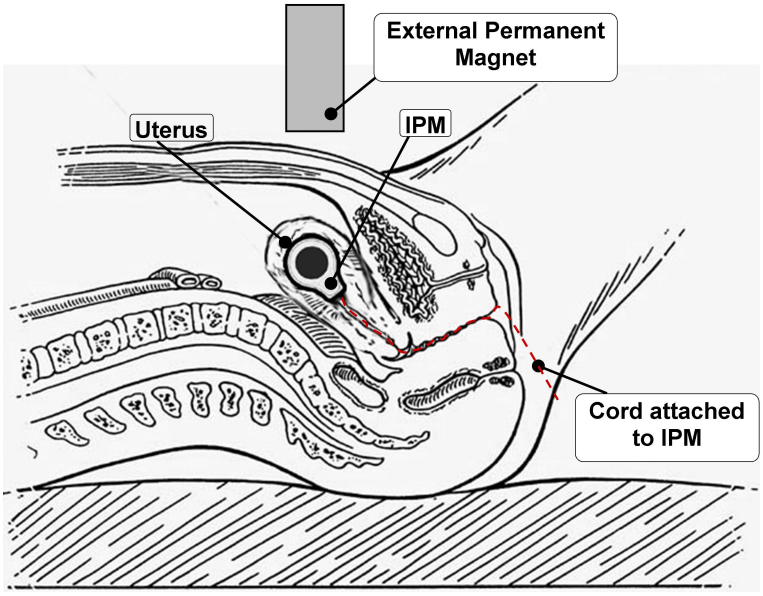

Figure 4.2: Position of IPM Inside the Uterus (Image adapted from Kavic and Levinson (1999))

The housing of the internal magnet was rapid-protoyped by SKEG Product Development in Cape Town, South Africa. After consulation with Gideon Els from SKEG, the wall thickness of the housing was fixed at 3 mm to maintain structural integrity of the housing in the uterus. The housing was then 3D printed using FullCure 720 polyethylene as a material. Figure 4.3 depicts the finished protoypes from SKEG.

Figure 4.3: Prototype of Internal Magnet Housing

4.2 Design of External Permanent Magnet

This section deals with the design and modelling of the external magnet which is the component that provides the actual working energy to manipulate the internal magnet and thus the uterus. As discussed in Chapter 3.1, focus will be put on design and modelling of a regular permanent magnet aswell as a permanent magnet with shielding. The purpose for modelling each of these concepts is to be able to discuss the viability of the design and whether the magnet is able to produce the desired lifting force of 1 N in an air-gap of 150 mm.

4.2.1 Permanent Magnet

Permanent magnets can be manufactured in various shapes and sizes. Some designs are tailored to achieve maximum contact force, whereas other designs are better suited to attracting a magnetic body over a certain distance. Parker (1990) states that to attract a magnetic body over a distance, you are concerned with maximizing the work of the system, hence maximizing the force

times the distance. To achieve this, a magnetic configuration is required that enables deep field pattern projection. Which it to say the poles of the configuration need to be far apart. Figure 4.4 depicts a graph of various magnets' pull strength versus the air gap length.

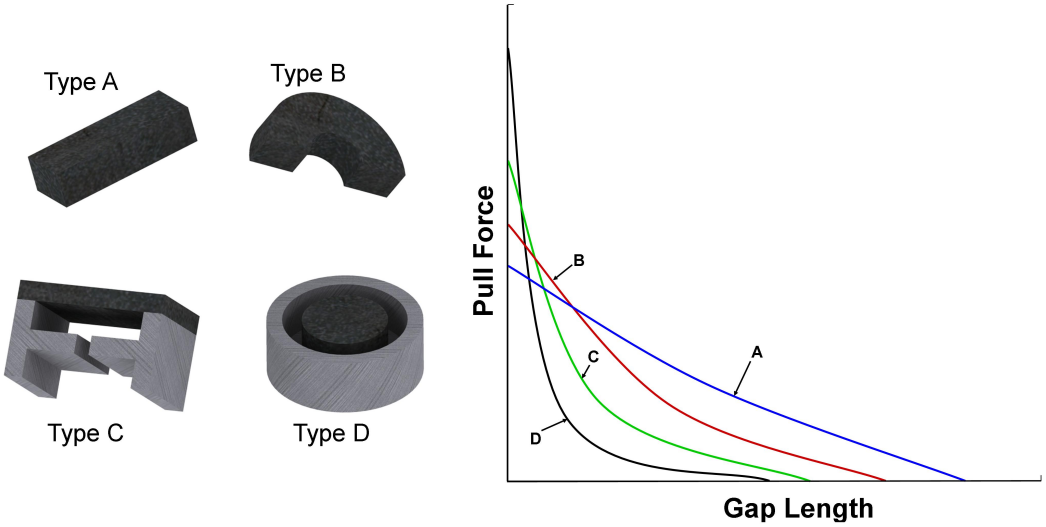

Figure 4.4: Magnet Array Setup and Functional Diagram (Adapted from Parker (1990))

It can be derived from Figure 4.4 Type A magnets exhibit the highest pull strength over a large air gap. This constrained the problem to looking at either cylindrical or cubic cores, where the length of the cores were considerably larger than the diameter or the width.

The second part of the process involved the selection of a suitable permanent magnetic material. As with the IPM selection, NdFeBr magnets have the highest remanant flux density, B_r, compared to any other material and are thus the obvious choice for a permanent external magnet.

To constrain the problem even further, Equations 4.1 and 4.2 used in the magnetic design industry, were applied to estimate the flux density at a certain distance, x, away from the core (Australian Magnetic Solutions; IBS Magnet; Integrated Magnetics). Equation 4.1 calculates the flux density at x for cylindrical magnets, where Equation 4.2 does the same for cubic magnets:

$$B_{x_{cyl}} = \frac{B_r}{2}\left[\frac{L+x}{\sqrt{R^2+(L+x)^2}} - \frac{x}{\sqrt{R^2+x^2}}\right] \tag{4.1}$$

$$B_{x_{cube}} = \frac{B_r}{\pi}\left[\frac{atan(AB)}{2x\sqrt{4x^2+A^2+B^2}} - \frac{atan(AB)}{2(L+x)\sqrt{4(L+x)^2+A^2+B^2}}\right] \tag{4.2}$$

where B_x is the flux density at the distance x, B_r is the remnant flux density at the exit pole of the magnet, R is the radius of the disk and L is its length. For the cubic magnet, A and B are the width and the breadth of the magnet respectively and, as in the cylinder, L is the magnet's length. In both cases x is the distance away from the pole constrained to the centre axis of the magnets.

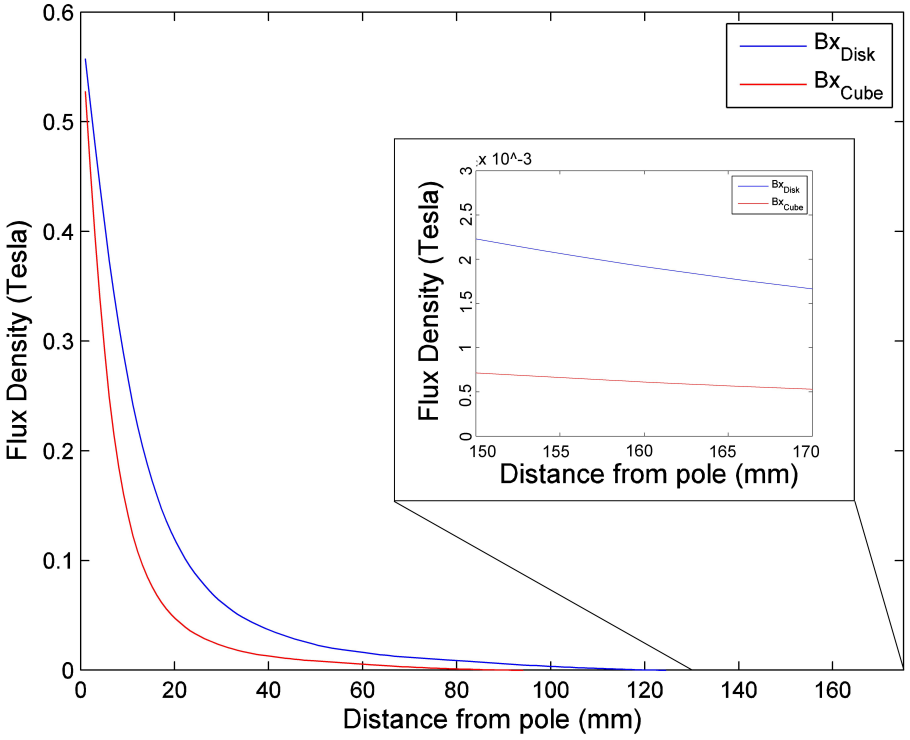

Figure 4.5: Flux density vs Distance in Cylinder and Cuboidal

Figure 4.5 depicts the flux density over the distance that the external magnet is expected to operate on while the graph insert zooms into the area of interest at a distance of 150 - 170 mm. Figure 4.5 is only used as a reference for this section of the report, to show the difference between the two equations at arbitrary dimensions of radius, R, and length, L. As depicted, there is a clear advantage of using a cylindrical magnet over a cubic magnet as the cylindrical magnet has almost double the flux density at any distance away from the pole. Furthermore, force is directly proportional to the flux density of a magnet, thus the cylindrical magnet is able to generate a higher pulling force.

To estimate the force on the magnet at the required distance away from the magnet, the empirical Equation 4.3 was used (Australian Magnetic Solutions, 2004).

$$F = 0.577B^2A \tag{4.3}$$

where F is the pulling force in pounds, B is the flux density at a certain distance from the magnet in kilo Gauss (kG) and A is the area of the magnet pole in inch^2. Area, A, can be rewritten as πR^2. Due to the fact that Equation 4.3 is in imperial units thus Equation 4.1 will have to be converted to imperial units in order to combine the equations.

The combined function is as follows:

$$F_x = 0.577\pi R^2 \left(\frac{B_r}{2} \left[\frac{L+x}{\sqrt{R^2+(L+x)^2}} - \frac{x}{\sqrt{R^2+x^2}} \right] \right)^2 \tag{4.4}$$

where F_x is the force at a certain distance, x, away from the magnet. Figure 4.6 depicts a graphical representation of the above equation over a range of radii and lengths. The distance x was fixed at 170 mm. Interestingly the force exerted by the magnet increases exponentially with only a minor increase in diameter size at a certain point.

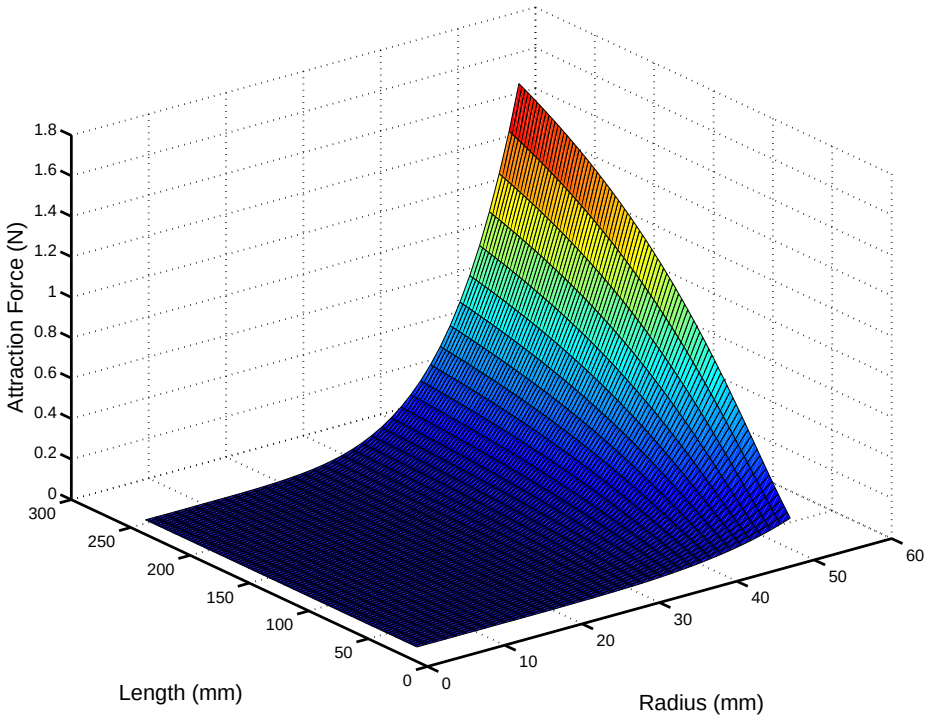

Figure 4.6: Force as a Function Height and Radius of a Magnet

Modelling the force using Equation 4.4 can give a good estimate of what the magnet dimensions, namely radius, R, and length, L, should be to achieve a force of 1 N at a distance of 150 mm away from the pole. Thus, a good initial guess for these dimensions could be made as a starting point for Finite Element Analysis (FEA) of the magnet problem. It has to be noted that Equation 4.4 assumes that the attracted object on which the force is acting is made from steel. Therefore the equation contains an intrinsic error if the properties of the attracted material vary greatly from those of steel and analysis through FEA is essential to arrive at a more accurate solution to the problem.
As mentioned in Chapter 2, Infolytica's MagNET v6 was used for the FEA analysis. A detailed look at how MagNET solves magnetic problems can be found in the Section 2.5.1. First the simulations had to be verified with a validation study to ensure the accuracy of the model and to be able to optimize mesh size and solving methods. A N38 NdFeBr magnet with a diameter of 30 mm and a height of 100 mm was chosen as the external magnet, as it was easy to procure. Its high B_r value also meant that it would induce a large attraction force on the spherical magnet, which could be measured experimentally. A spherical magnet with a diameter of 20 mm was chosen as the internal magnet. The problem was solved numerically in MagNET using an axisymmetric method, meaning only a quarter of the problem had to be modelled which could then be solved in two dimensions instead of three. As a result, solving time and computer resources were reduced. Figure 4.7(a) depicts the layout of the design in three dimensions, whereas Figure 4.7(b) depicts the model setup in the MagNET solver.

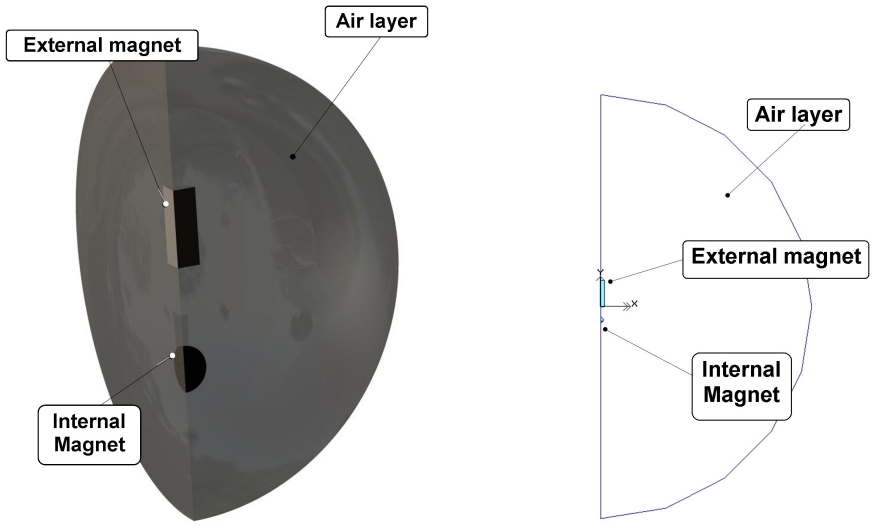

(a) Axisymmetric Simulation Model of Magnet

(b) MagNET Model

Figure 4.7: Axisymmetric Model Description

The environment meshing was an ongoing process which needed to be validated before a judgement on the model's accuracy could be passed. Since the simulation models for this problem consisted only of non-current carrying elements MagNET implements the *Maxwell stress* method to calculate forces on the bodies. This method involves force computations over the layer of air elements that are directly in contact with the body. As a result, this method can lead to error computations in the mesh due to the fact that the actual geometry of the body is ignored, thus features like holes or surface imperfections (sharp edges) are not taken into consideration. To measure the degree of error, an error plot was created in MagNET. Such a plot is dimensionless and describes the error of the model by measuring discontinuities in the magnetic flux and plotting them as a colour gradient on a scale of zero to one. Figure 4.8 depicts such a plot. For the magnetic system, the meshsize, h-adaption and polynomial order of the solver were refined until the residual error was 0.112 N and which was confined to a small region around the top and bottom circumferential edge of the cylinder. This can be seen in Figure 4.8. An error plot over the central cylindrical axis is depicted in Figure 4.9. The sharp spike represents the spherical magnet, whereas the two smaller spikes represent the top and bottom of the cylindrical magnet. As can be seen, the error plot on the y-axis is sufficiently far below the maximum error.

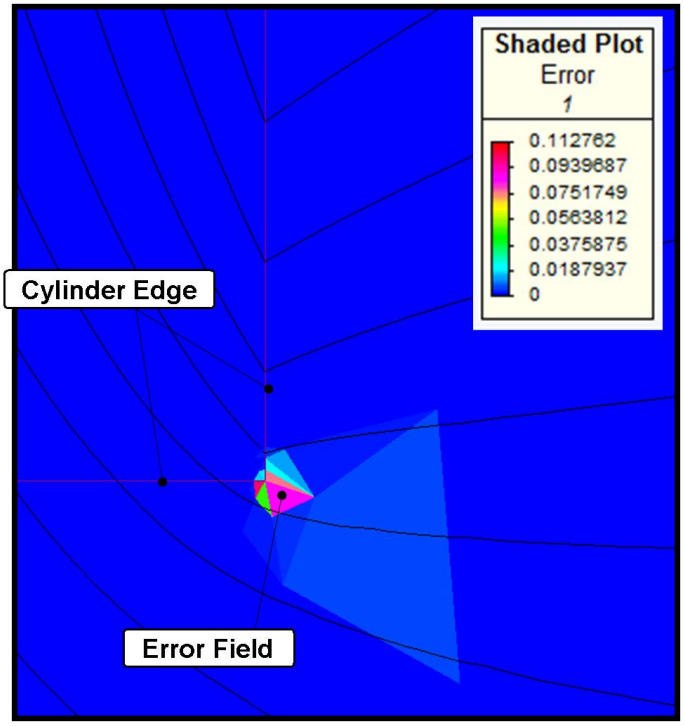

Figure 4.8: Error Field Plot of Cylindrical Circumferential Edge

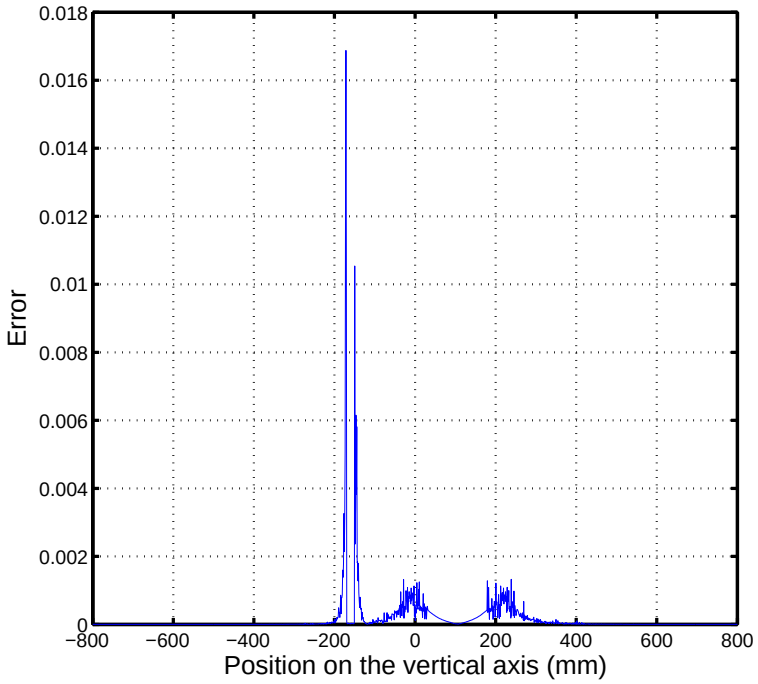

Figure 4.9: Error Plot of the Vertical Cylindrical Axis

4.2.2 Validation

A validation study needed to be performed to accurately gauge the simulation performance and accuracy. Figure 4.10 depicts the setup of the test rig used to measure the force from the external magnet on the internal magnet. The load cell used was a high-accuracy HBM PW6CMR/20KG load cell, with a sensitivity of 2.2 mV\V and a maximum measurable load of 20 kg. It was mounted on an adjustable arm, as depicted in Figure 4.10, to enable the load cell to always measure the load perpendicular to the bottom surface of the external magnet. As the arm is always rotated with the movement of the external magnet, the force should always be similar around the circumference of the arch. The internal magnet, encased in its housing, was attached to the load cell via 2 mm thick wire. The load cell was attached to a Spider8 instrument amplifier which was in turn connected to a laptop, via USB, running the data acquisition program Catman®Easy by HBM.

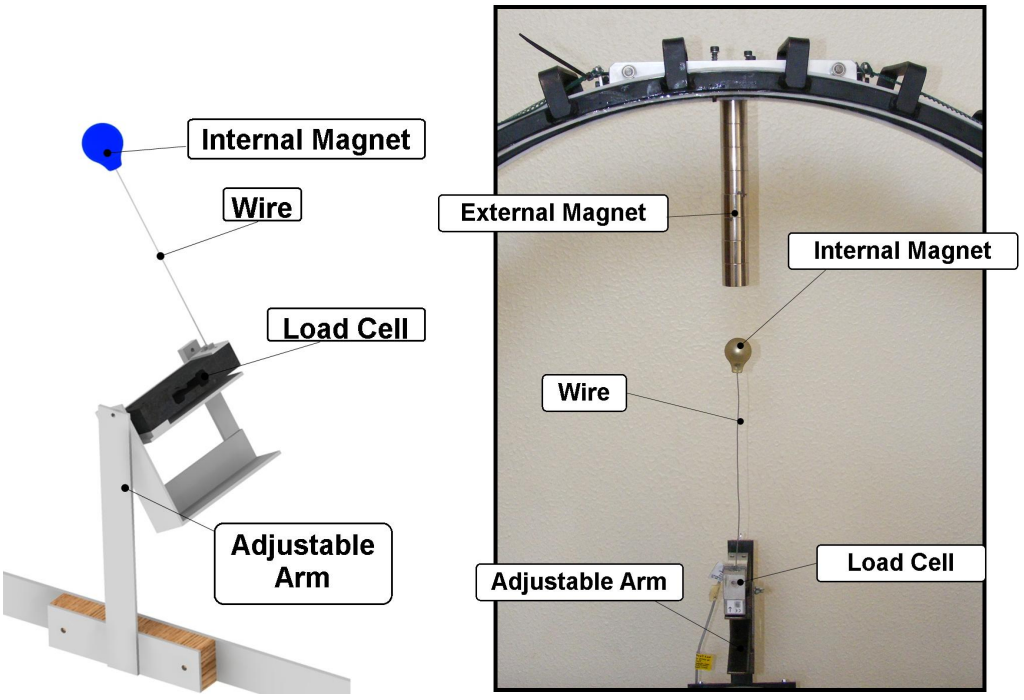

(a) Test Setup Design (b) Experimental Test Setup

Figure 4.10: Load Cell Test Setup

As Catman®Easy had no database record of the chosen load cell, a sensor identification parameter had to be created. Next, the load cell had to be calibrated. A linear calibration was done between 1 kg and 2 kg, using a 1 kg and a 2 kg weight, as the force on the IPM was expected to be no more than 15 N. Before the 1 kg weight was attached, the load cell was zeroed to exclude the force of its own weight on the reading. After this the weights were successively attached to the load cell and the raw data voltage output for each weight was recorded. A linear calibration could then be achieved by including the measured values in the sensor's calibration curve. After testing, the load cell correctly recorded both weight values to within a range of 15 grams of the true weight. This was deemed sufficient for data acquisition. The next step was to create a testing protocol. This protocol required the load cell to be zeroed before each new set of measurements was made. The 1 kg weight was attached to the load cell after each set to check for any deviations. Lastly, each set of data packets comprised of three measurements at the same distance which were then averaged to obtain a rounded result. Testing of the force was done in the vertical, as depicted in 4.10(b), to achieve maximum correlations with the simulation data. Furthermore, testing was done over an air-gap ranging from 20 mm to 40 mm which was increased in increments of 5 mm. Figure 4.11 depicts an air-gap measurement. As mentioned, at each distance, three individual load measurements were taken and averaged.

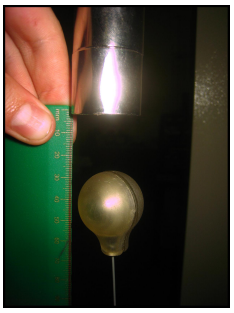

Figure 4.11: Air-gap Measurement

Finally, the experimental and simulation results were plotted and compared. Figure 4.12 depicts the experimental and the simulated force measurement over distance. As expected, the simulation results correlated very closely to the experimental results. The simulation was validated over this short range of values because the force was expected to be strongest there and it was expected to correlate well with simulation data. The model is valid for larger distances between the magnets as is documented in Chapter 5.2 where the model was validated up to a 110 mm air-gap with a magnet diameter of 30 mm and height 200 mm.

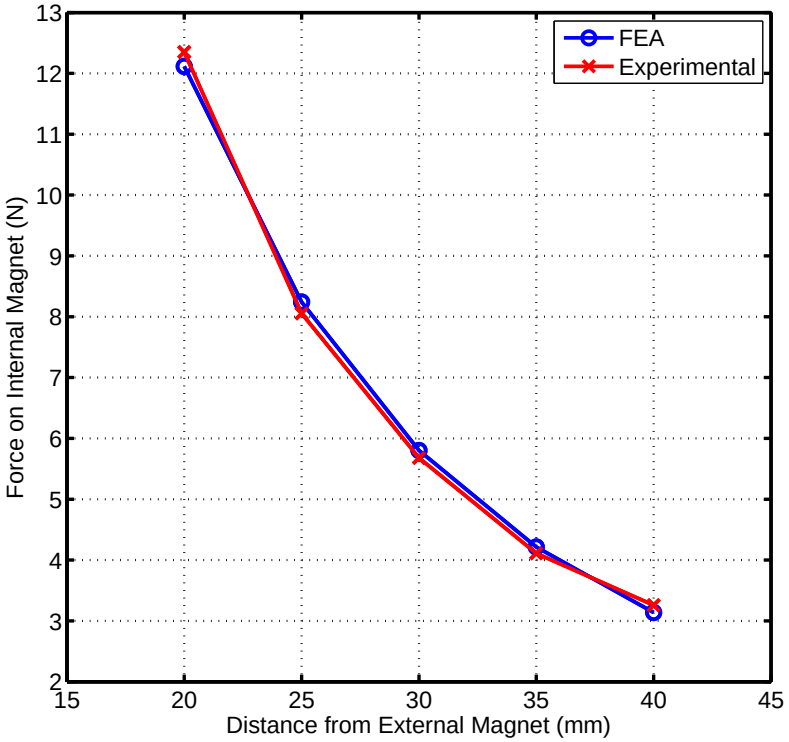

Figure 4.12: Validation of the Simulated Model

To quantify the error between the experimental and simulation data, a MAE (Mean Absolute Error) analysis was performed. The MAE measures the average magnitude of the errors and accuracy in a set of continuous variables. Equation 4.5 is the MAE equation.

$$MAE = \frac{1}{n}\sum_{i=1}^{n} \mid f_i - y_i \mid \tag{4.5}$$

After inserting the simulation and experimental data into above equation an error of 0.153 N was calculated. This was deemed accurate enough, as a design buffer bandwidth was already calculated into the desired mass that must be lifted. Therefore, the error would affect the final result insignificantly and the simulation parameters were finalized as follows:

Cylindrical Magnet Mesh Size: 0.3 mm
Spherical Magnet Mesh Size: 0.3 mm
Air Field Mesh Size: 0.5 mm
h-adaption: 25% with a tolerance of 0.001%
Polynomial order: 4

The rest of the settings were kept at their default. To conclude, the validation process made the simulation model valuable for designing magnets without testing. Design could now continue to estimate the dimensions of the final external dimensions. The final design of the external magnet is discussed in Chapter 5

4.2.3 Permanent Magnet with shielding

Shirazee and Basak (1995) describe a method of using shielding as a conduit to guide magnetic flux lines and expel them further into the large air-gap region existing between the EPM and the IPM. Furthermore, the shield prevents flux lines from being expelled at the top most part of the magnet, essentially wasting energy. At the same time this effect increases the safety of the system as the shielding drastically minimizes the attraction force at the top of the magnet, preventing accidental attraction of ferromagnetic objects. Unfortunately, their research in this field was not well documented and a simulation study into the design geometry of such shielding had to be conducted. Magnetech, a company specialising in magnetic design, from Somerset West, South Africa, suggested design equations that they utilize in simple magnetic assemblies to shield magnets and direct a magnetic field. Equation 4.6 specifies the shield base diameter as a function of the core diameter of the external magnet.

$$ShieldBaseDiameter = \frac{CoreDiameter}{0.6} \tag{4.6}$$

Also, the shield thickness is specified by a function. Equation 4.7 depicts the relationship between the shield thickness and the shield base diameter.

$$ShieldThickness = 0.14 \times CoreDiameter \tag{4.7}$$

Subsequently these design equations were used as a starting point for the experimental analysis. As with the design for the permanent magnet and the electrical magnet, a Microsoft Excel Visual Basic program was written which produces a DXF file that could be imported to Infolytica's MagNET for analysis. The only input requirements from the user were the core diameter and the shield height. A simple simulation was run to prove the concept and compare the results obtained to a similar magnet without the shielding. Figure 4.13 depicts the flux plot of both models to show the effect that shielding has on the magnetic setup. Surprisingly, the shielded magnet also increased the force vector on the external magnet at a distance of 30 mm from the unshielded force vector of 5.94 N to 5.99 N. The magnets both had a diameter of 30 mm and were 200 mm in height. During the course of this thesis, the scope limited the research on magnetic shielding to a comparative simulation study as a proof of concept. As per Figure 4.13 it can be seen that the results would definitely warrant further investigation.

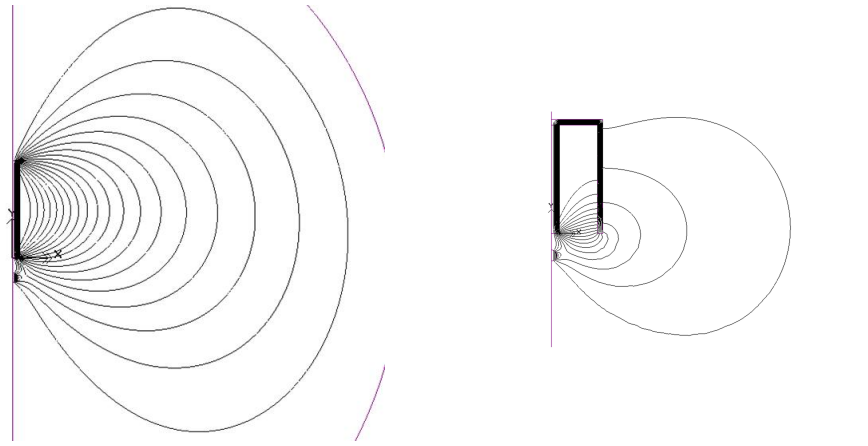

(a) Unshielded Flux Plot (b) Shielded Flux Plot

Figure 4.13: Comparison of Flux Plots

4.3 Design of the Actuator

The actuator system was designed after the selection of the external magnet. This was necessary to allow for accurate weight values needed in the torque calculations. As explained in Section 3.3.5 the cart-on-arch concept was chosen because of its simplicity, lack of high powered electrical equipment, its light weight and its ability to easily manipulate the external magnet. This section attempts a structural decomposition of the entire assembly to explain the design and function behind each individual part.

4.3.1 Arch

The arch was designed using two sections of 19.2 mm wide square steel tubing which were bent to a radius of 510 mm. The sections were then connected in parallel via steel brackets. Figure 4.14 depicts the arch design.

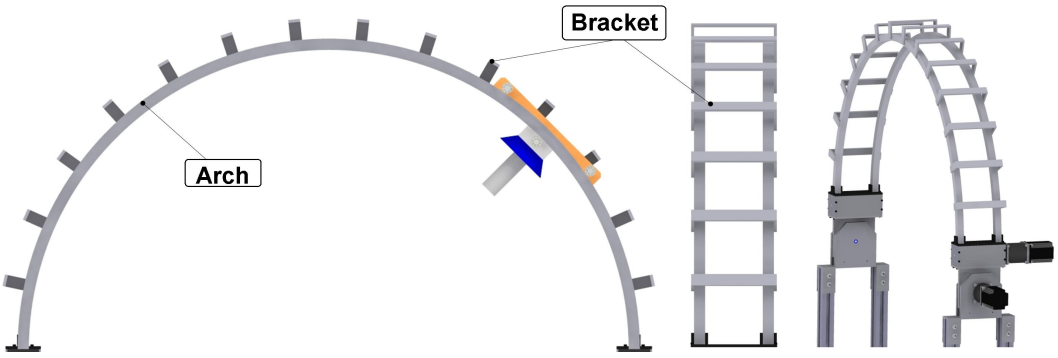

Figure 4.14: Arch Design (Front, Side and Isometric view)

Square tubing was used to act as a guide for the belt pulling the cart over the arch. In retrospect it must be mentioned that the arch could have been manufactured from aluminium tubing instead of steel to reduce the weight of the arch. A recommendation for the second prototype would also be to remove a number of the brackets as the structure would still maintain stability.

4.3.2 Pulley System

To drive the cart, a pulley and belt system was designed. Pulleys were mounted on either end of the arch to enable a belt to pull the cart in a clockwise and anti-clockwise direction over the square tubing, which facilitates lateral movement of the uterus. The pulley, shaft and housing were manufactured from aluminium to reduce weight. Figure 4.15 depicts the pulley system design.

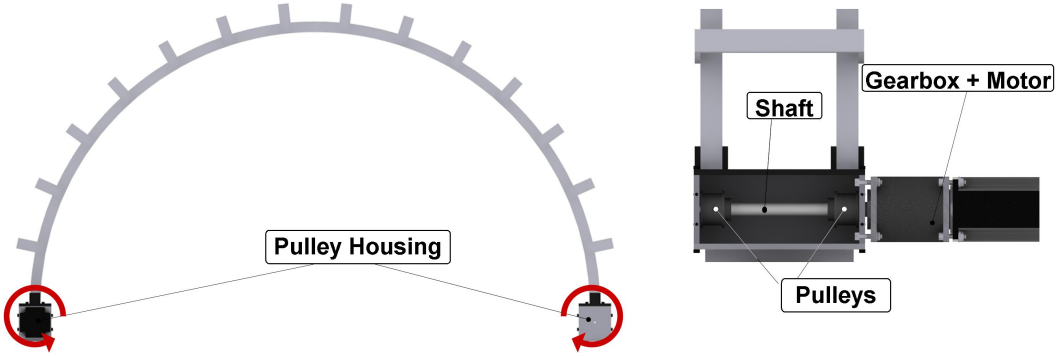

Figure 4.15: Pulley System Design (Front and Sectioned view)

The sectioned view depicts the driving pulley system with attached gearbox and motor. Design of the driven pulley system is similar but does not feature a motor coupling on the shaft. Calculations for the pulley diameters can be found in Section 4.4.1. Manufacturing was done by Fabrinox (Fabrinox, Paarl, South Africa).

4.3.3 Arch Actuator

The arch actuation system was designed to tilt the arch 30° in a clockwise and counterclockwise direction. This in turn manipulates the internal magnet and thus facilitates antiversion and retroversion of the uterus. Figure 4.16 depicts the arch actuator design.

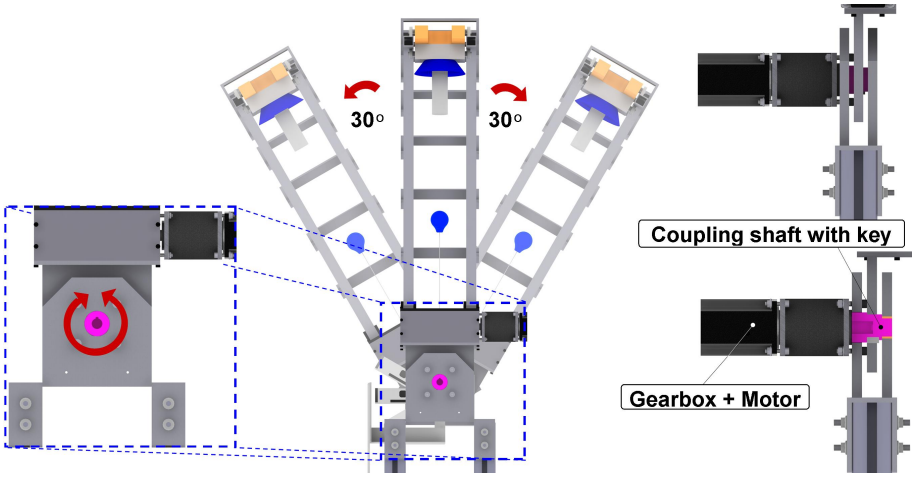

Figure 4.16: Arch Actuator Design (Cut-out section, Rotation, Sectioned sideviews

The 30° limitation on the actuator rotation angle was imposed by limited operating theatre space. Even after reaching its rotation limit, the surgeon should still be able to comfortably use all the necessary tools and laparoscopic ports available.

4.3.4 Cart

The most important part of the mechanical assembly is the cart to which the external magnet is connected. A lightweight design was desired as to reduce the load on either motor driving the cart and the arch. Consequently aluminium was selected as manufacturing material. Figure 4.17 depicts the cart design.

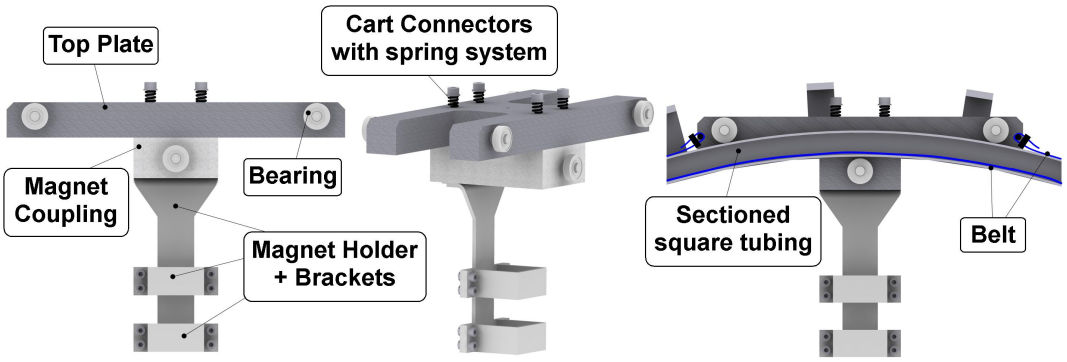

Figure 4.17: Cart Design (Front view, Isometric view, Sectioned Arch Assembly view)

As the arch rails were not perfectly smooth and symmetrical the design of the cart system had to be such as to adapt to the rail imperfections. The isometric view in Figure 4.17 depicts the spring system with which the magnet coupling was attached to the top plate of the cart.

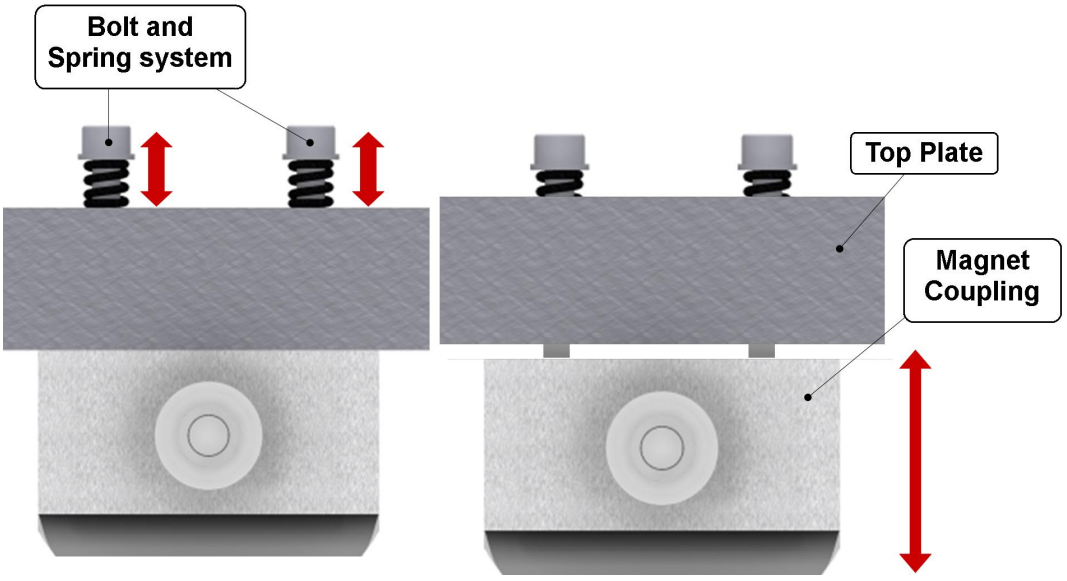

Figure 4.18: Spring Displacement System for Cart

As per Figure 4.18, the magnet coupling is fitted with threaded holes to which bolts are connected running through the top plate. As a result the magnet coupling has a significant tolerance for movement in a downward direction. To limit this movement further, springs with a high spring coefficient were introduced between the bolt head and the top plate. Consequently this limited movement slightly, but enabled the cart to adapt to the imperfect rail circumference of the arch.

The magnet holder and bracket attached to the bottom plate were designed to be adaptable to a number of magnet diameters. The inside of the bracket was lined with rubber to grip the magnet without damaging its surface. Furthermore, the brackets can be easily unfastened to allow the external magnets' distance from the internal magnet to be variable.

4.3.5 Support Structure

The structure was designed with portability in mind. BoschRexroth™ aluminium extrusions were used as they are easy to assemble, lightweight and sturdy once assembled. In addition, the whole structure is mounted on lockable wheels to stabilize it during a surgery. Afterwards it can easily be transported and stored. Figure 4.19 depicts the structure design.

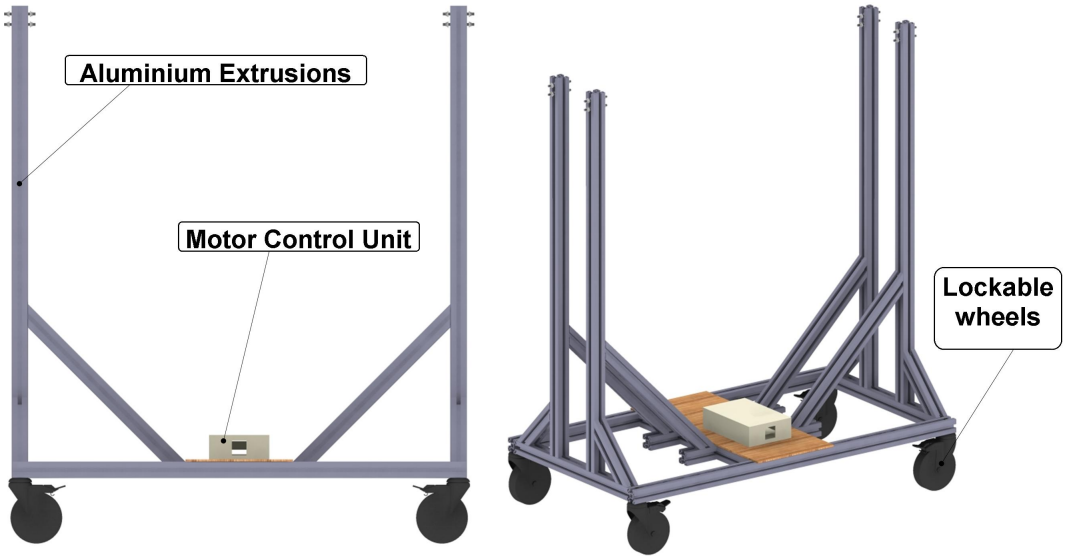

Figure 4.19: Structure Design

Housed on the base of the structure is the motor control unit which is responsible for manipulation of the arch and cart. Furthermore the power supply was also housed on the base. This positions it safely out of range during surgery to prevent accidental damage to the control unit and minimize the risk of potential electrical injuries.

4.3.6 Manipulator Assembly

The final section of the manipulator design covers the entire assembly of the uterine manipulator. Figure 4.20 depicts an isometric view of the total design with descriptions of each segment.

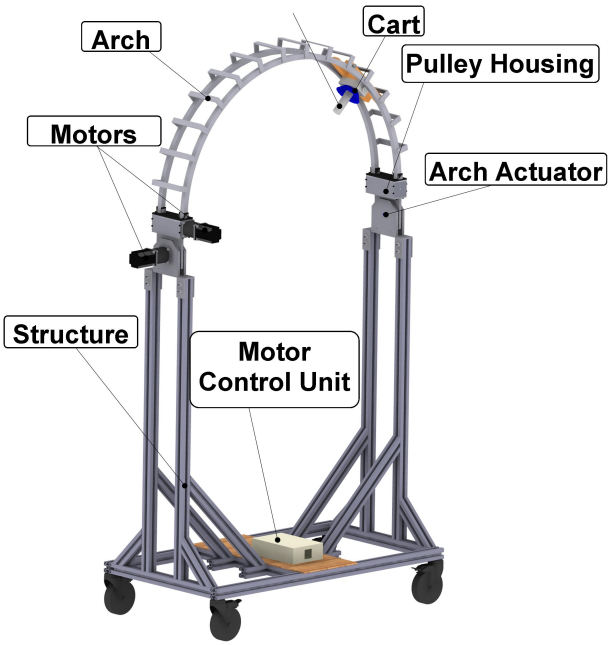

Figure 4.20: Total Assembly

The manipulator was designed to take up minimal surgical theatre space, with the width of the arch being only 130 mm. Furthermore, the manipulator adheres to all the limitations imposed on it by previous manipulator designs summed up in Table 2.1. Ease of use of the device is paramount and it requires very little training to operate. Unfortunately, due the device being an external manipulator it has to be noted that the antiversion/retroversion angle, explained in Figure 2.2, was limited to 60°. It would be possible to design the arch for a larger manipulation angle, but this would greatly inhibit operating space and access to laparoscopic ports. The next section will cover the actuating parts necessary to achieve the required movement of the device.

4.4 Motor Selection and Electronic Design

This section deals with the motor selection and the design selection of the electronic equipment necessary to control the motors. Included in the design are the torque calculations and the electronic schematics.

4.4.1 Motor Selection

The following section deals with the selection of motors to drive the cart system as well as the rotating arch. This part of the design process was only possible after the design of the external magnet, the shielding and the cart, as these parts contributed significantly to the bulk weight of the device. In

order to calculate the maximum torque for the cart pulley system, a simple model was created which could be used to accurately predict the torque. A 25 mm diameter, 27T5/25.2 aluminium pulley, with a pitch of 5 mm, from RS Components was selected as the driving pulley. Figure 4.21 depicts the pulley moment diagram and the position of the cart in which the motor will have to do maximum work.

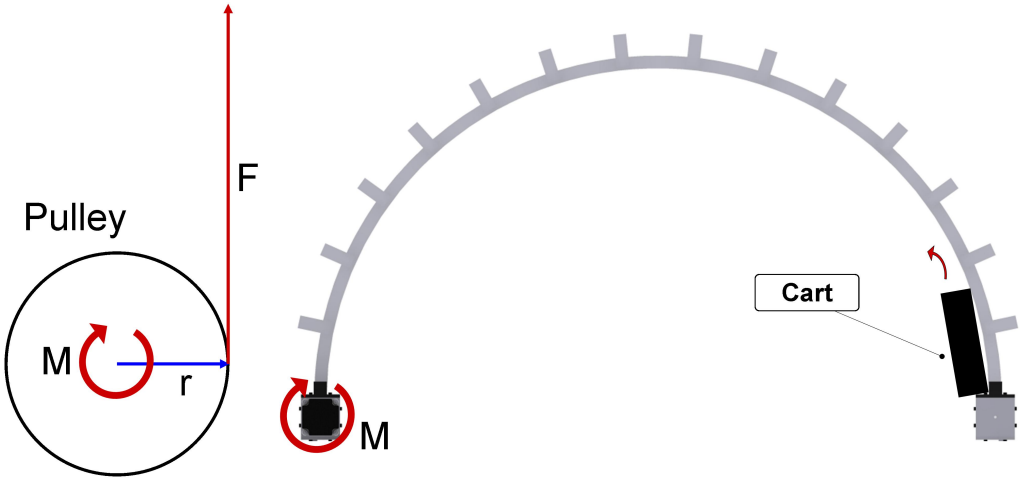

Figure 4.21: Pulley Moment Diagram

The combined mass of the cart and external magnet was measured to be 1.5 kg. Thus all the constants to solve Equation 4.8 are known.

$$M = F \times d \tag{4.8}$$

By inserting the known constants we can solve latter equation for M, where $d = r = 0.0125$ m and $F = m \times g$.

$$\begin{aligned} M &= 1.5 \times 9.81 \times 0.0125 \\ &= 0.184\, N{\cdot}m \end{aligned} \tag{4.9}$$

The solution is a very low torque of 0.184 $N{\cdot}m$, also the pulley was expected to rotate at very low speeds and thus the effects of dynamic were deemed negligible. Consequently a 57SH76 Bipolar stepper motor from RS Components was selected as the pulley driving motor. The motor has a maximum dynamic torque of 1.4 $N{\cdot}m$, a maximum holding torque of 1.89 $N{\cdot}m$ and a step angle of 1.8°. A stepper motor was selected due to the fact that the cart position needs to be held, hence a holding torque is required. Using a DC motor was a possibility but that meant incurring the added cost of a magnetic brake and positional feedback sensors for the system. To drive the cart, a T5 timing belt from Transdev with a pitch of 5 mm was used. As the belts were only available in maximum lengths of 1.7 m they had to spliced to cover the circumferential distance of 3.32 m around the arch.

After installation and testing of the pulley-belt system it was found that the motor had difficulties driving the cart. This was attributed to friction between the belt and the arch surface which was thought to be negligible during modelling. It was decided to install a IP057-M02 planetary gearbox from McLennan Servo Supplies Ltd to increase the torque. This gearbox had a gear ratio of 1:25 with a maximum operating torque of 25 $N{\cdot}m$, which was more than sufficient to draw the cart over the arch.

The next part of the design process required the modelling of the rotating arch system. Figure 4.22 depicts the moment diagram for the arch and the solution after rotation of the arch through angle Θ.

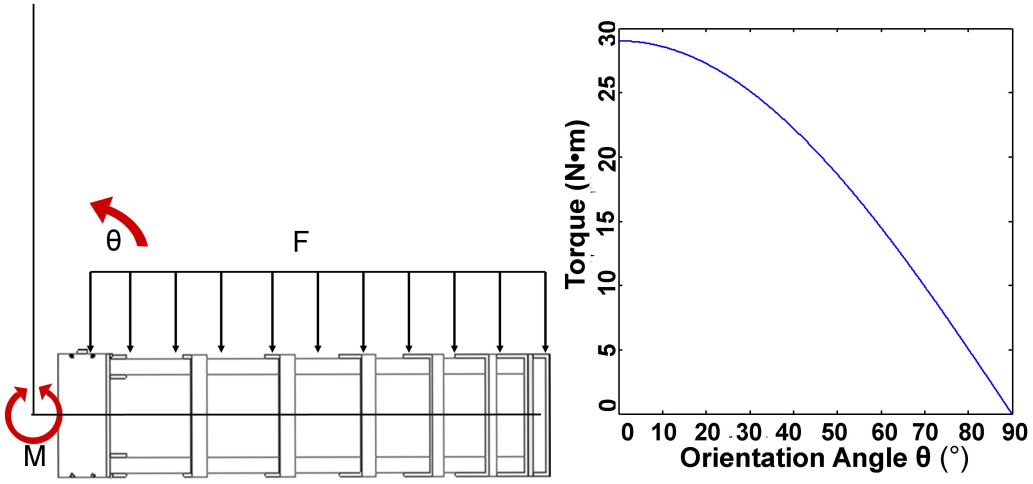

Figure 4.22: Arch Moment Diagram and Solution Graph

As the arch rotation is constrained to a 30° rotation in the clockwise and counterclockwise direction from the vertical (refer to Section 4.3.3) the torque at that angle could be read off from Figure 4.22. Matlab was used to simulate a simple model of the arch rotating 90° about the origin. To calculate the torque all the individual masses of the parts on the arch were programmed into the torque model. The cart and the magnet were assumed to be at the maximum distance of 260 mm from the origin, whereas the centre of mass was found for the arch and arch brackets. From the graph it could read off that roughly 15 $N{\cdot}m$ of torque was required to rotate the arch 30° in either direction from the vertical and hold it at that position. Consequently as for the pulley system a 57SH76 Bipolar stepper motor, with holding torque of 1.89 Nm, from RS Components was selected along with an IP057-M02 planetary gearbox from McLennan Servo Supplies Ltd with a maximum operating torque of 35 $N{\cdot}m$. After assembly and testing it was found that the motors performed to expectation.

4.4.2 Electronic Design

The following section will deal with the electronic design which was necessary to be able to control the motors for the arch and the pulley-belt system. After selection of the motors, suitable motor drivers had to be found, including a controller which would drive both actuating parts at the required accuracy. An Arduino Mega 2560 microcontroller board was chosen as the primary driver. The board is based on the ATmega8U2 chipset. It was selected because it has 54 digital I\O pins of which 14 can be configured as pulse-width modulating outputs. Furthermore, the board has 14 analogue pins, an onboard 256 kB flash memory, and in addition, it can easily be programmed via a USB port. The selection of the Arduino Mega 2560 made the design very modular, which greatly simplified the addition of sensors or actuators to the existing design.

An MSE570 Evo 2, 3.5 Amp\phase Bi-polar stepper motor drive was chosen as the driver for the arch actuator. The input to this board is 15-48 Vdc depending on the motor torque requirements. The driver can drive the stepper motor at either half step or full step and the speed of the motor is controlled by a clock pulse input from the microcontroller. Since the torque load on the pulley driver motor was significantly less than for the arch motor, a less powerful stepper driver board could be selected. As there were no local suppliers for smaller stepper drivers in South Africa, a board was ordered from China via E-bay. The board has a 2 A\phase output as well as speed and direction control via an external controller. Figure 4.23 depicts the schematic of the entire system.

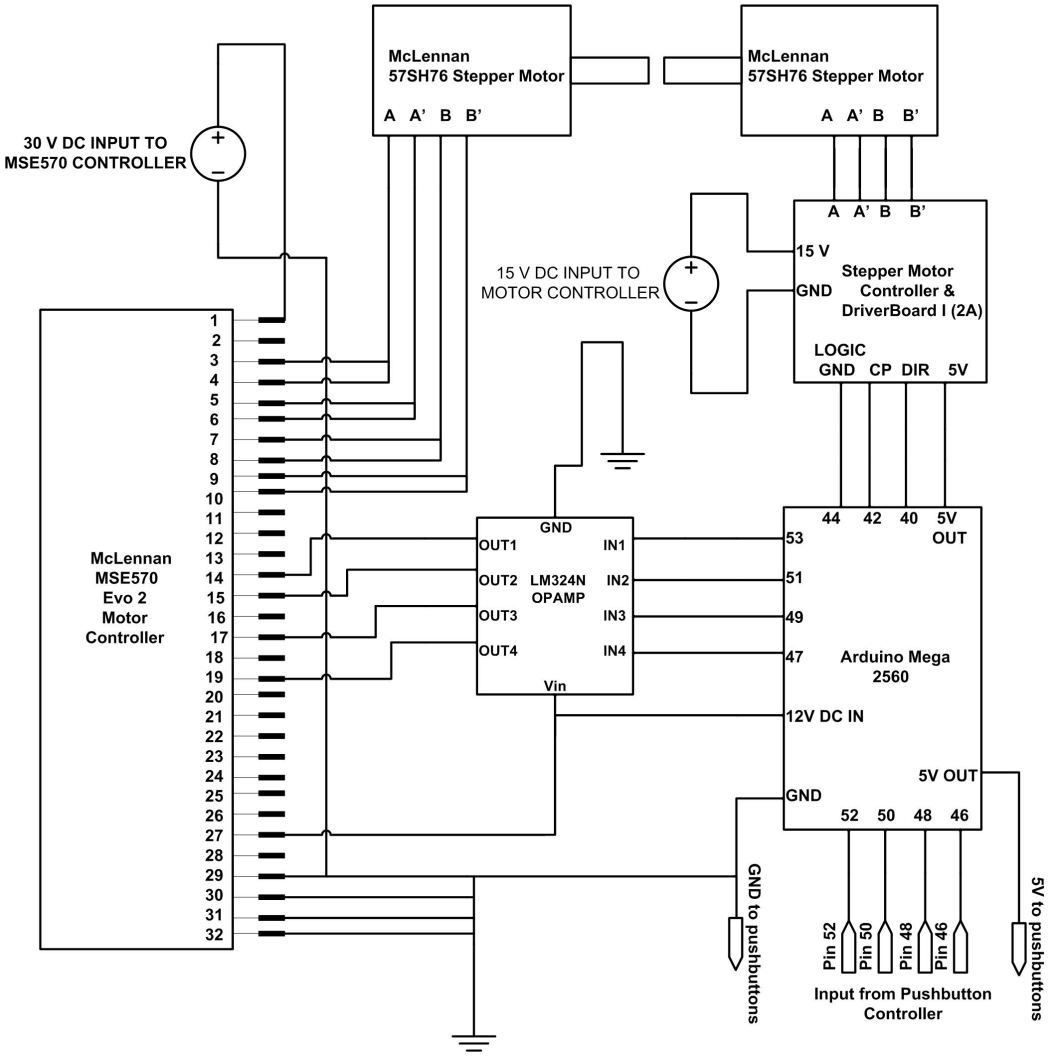

Figure 4.23: Electrical Wiring Diagram for the Entire System

Unfortunately, an Operational Amplifier (Op-Amp) had to be used to bridge the connection between the MSE570 Evo 2 and the Arduino microcontroller. This was due to the MSE570 Evo 2 having a logical input "HIGH" that is set between 9 - 13 Vdc but the Arduino only being able to provide a maximum output of 5 Vdc. An LM324N Op-Amp was designed to boost the signal from 5 V to 11.5 V with the help of the non-inverting Op-Amp Equation 4.10

$$\frac{V_{out}}{V_{in}} = 1 + \frac{R_F}{R_S} \tag{4.10}$$

where V_{out} and V_{in} are the input and output voltages of the opamp terminal, R_S is the source resistor and R_F is the feedback resistor. Inserting values into Equation 4.10 leads to

$$\begin{aligned} \frac{11.5V}{5V} &= 1 + \frac{R_F}{R_S} \\ 1.3 &= \frac{R_F}{R_S} \end{aligned} \tag{4.11}$$

Thus to satisfy Equation 4.11, R_S can be 1 kΩ and R_F can be 1.3 kΩ. Figure 4.24 depicts the schematic layout of the Op-Amp design where a R was simply an input resistor to limit voltage and was selected to be 1 kΩ.

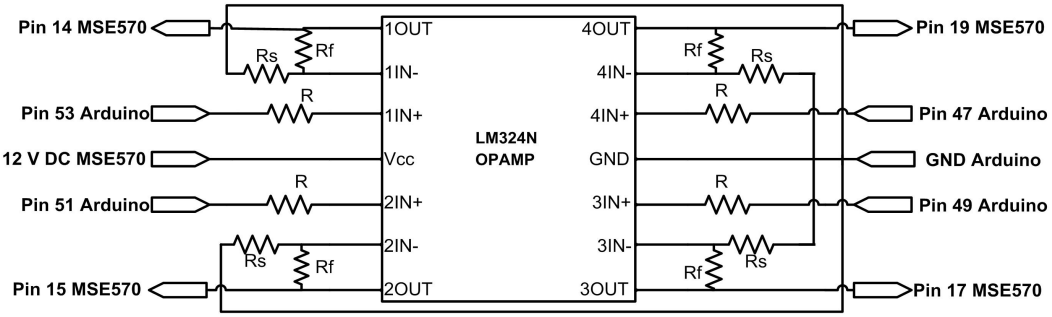

Figure 4.24: LM324 Op-Amp Wiring Diagram

The last section of the electronic design section deals with the design of the pushbutton controller to actuate the motor at will. To make the design as simple as possible, a four pushbutton design was chosen which enables the two motors described in Section 4.4.1 to rotate in either a counterclockwise or a clockwise direction. The buttons are wired in such a way, that if the button is pressed, it pulls the input pin of the Arduino high, which can then be registered as a button press in the software. Once the button is depressed, the input pins were pulled low and registered as such in the software. Figure 4.25 depicts the schematic of the pushbutton pad.

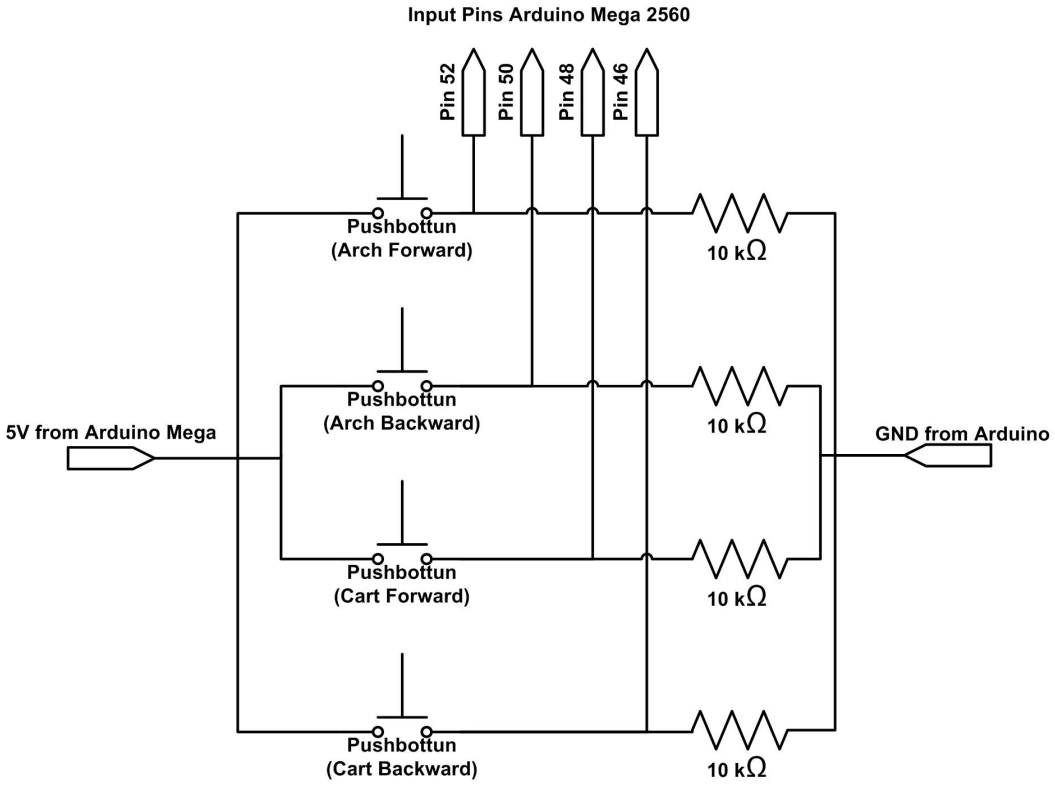

Figure 4.25: Pushbutton Wiring Diagram

4.4.3 Summary

To summarise up the Motor Selection and Electronic Design section, it can be said that all the components selected satisfy the design of the device and performance of each component was as expected. If necessary, sensors or different types of actuators can easily be added to the design as the device was intended to be modular. Chapter 5 will focus on testing the device experimentally and analyzing the results.

Chapter 5

Experimental Results

This section deals with the results from the design and modelling section. The magnetic design as well as the actuator design will be discussed.

5.1 Final Actuator Results and Prototype

The cart-on-arch actuator system performed as expected with a lateral rotation of $\pm 70°$ in the transverse plane and a $\pm 30°$ rotation in the anterior sagittal plane, as depicted in Figure 5.1. Motor and gearbox selection was adequate to effectively manipulate the arch and cart. Operation of the motors via the push-buttons was seamless which meant position could effectively be established and controlled.

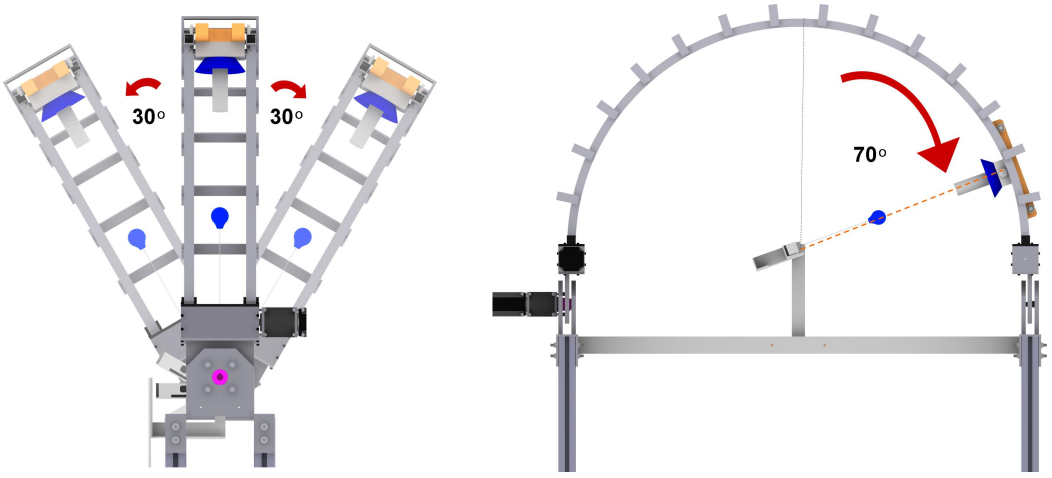

Figure 5.1: Actuator Rotation Limits

Figure 5.2 depicts the final prototype assembly including the internal and external magnets to depict the experimental range of rotation. Both stepper motors and gearboxes had enough torque to manipulate the arch and cart with

ease. Since the motor controller box was fitted with a 12 V fan, the stepper drivers were kept under maximum operating temperature of 80°C.

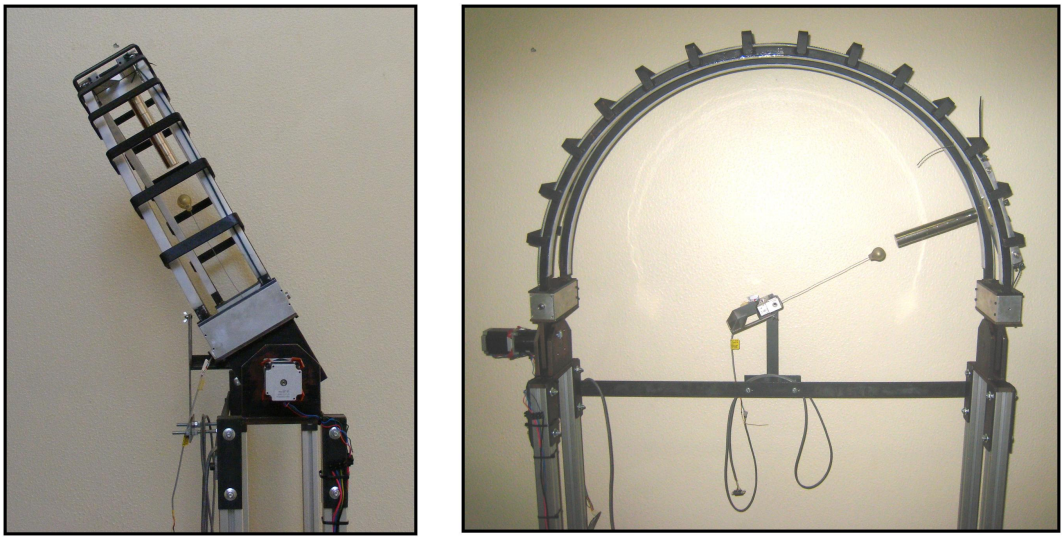

Figure 5.2: Prototype Rotation Limits

In conclusion, the device performed as designed. It must be noted that the design of the arch actuator and of the arch itself can be improved by manufacturing the parts from aluminium instead of steel. Firstly, this would decrease the total weight of the system and secondly, steel is ferromagnetic and influences the magnetic flux of the external magnet to some extent. As aluminium is diamagnetic it remains relatively inert to a magnetic field exposure.

5.2 External Magnet Simulation and Experimental Results

The final prototype external magnet had a diameter of 30 mm and a height of 200 mm. The simulation and experimental results are depicted in Figure 5.3. This magnet was selected as it was the largest N38 NdFeBr magnet currently available in South Africa. Unfortunately larger diameter NdFeBr magnets were only available from China. In this case they would have to be custom made and the manufactures, Ningbo Ketian Magnet Co. Ltd, required a minimum purchase quantity of 100 magnets which would end up costing more than the budget available to the thesis. The final experimental results were obtained through the same process as in the validation study and the experimental protocol was identical to that of Section 4.2.2. The only difference in procedure was in the fact that the magnetic attraction force was tested over a range of 20

mm to 110 mm in increments of 5 mm. Lastly, the magnetic attraction force was tested in the vertical as this position correlated with the simulation data.

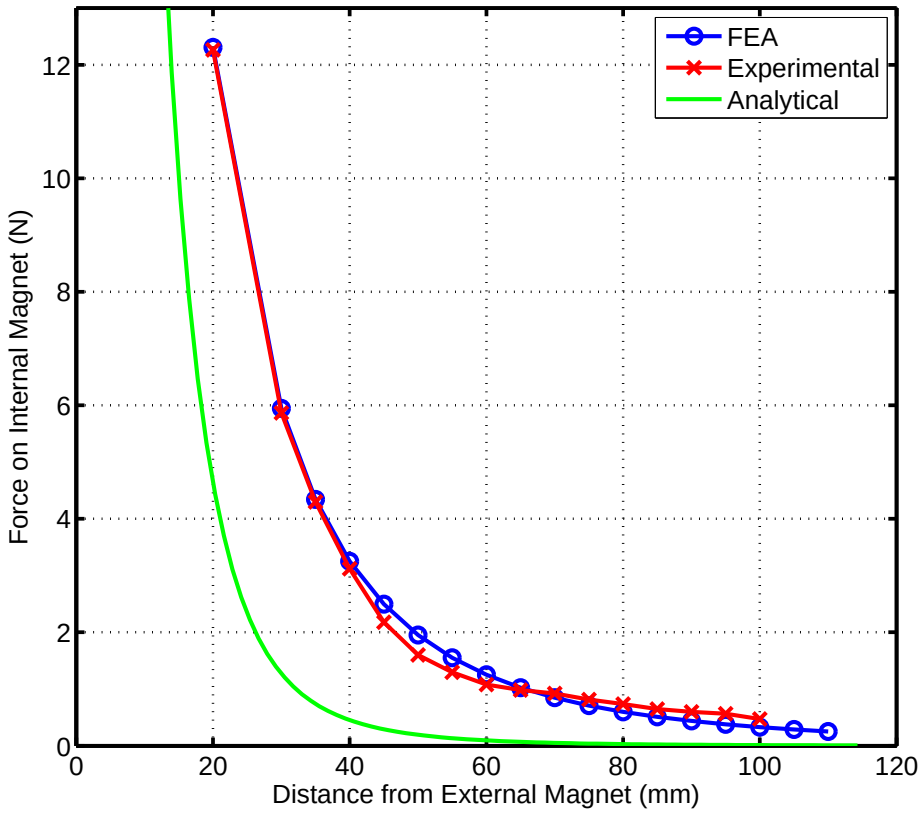

Figure 5.3: Final Magnet Prototype (d = 30 mm, h = 200 mm) Correlation factor r = 0.9984

As can be seen from the figure, the analytical calculations, from Equation 4.1, are inaccurate and can thus only be used as an estimate for the magnet dimensions necessary. The setup was simulated in MagNET according to the parameters fixed in the validation of the magnetic model. It can be seen that the experimental data deviates slightly from the simulation results, especially at larger air-gaps. The MAE was calculated to be 0.1492 N which was less than the MAE of the validation model. The error might be attributed to the meshing error or perhaps the influnce of the steel arch potentially strengthening the field. No concrete cause of the deviation could be found though. Nevertheless, as the simulation results are slightly less than the experimental results, the design of the magnet in simulation will always be sufficient in a real world application as the risk of under design is minimized. In addition the correlation factor, r, of the experimental and simulation data is 0.9984. This

means the experimental data agrees strongly with the results attained through the simulation. A final simulation to determine the magnet diameter and the height of a magnet that has the potential to attract the internal magnet with a force of 1 N over a distance of 150 mm was completed. The result was a magnet with a diameter of 110 mm and a height of 200 mm. The resultant design had an attraction force of 1.532 N. This model is expected to be a successful external magnet and will still have to be verified experimentally.

In conclusion it can be said that the design of the external permanent magnet was a success at proving the concept of external magnetic uterine manipulation. The device will still need the stronger magnet mentioned earlier to function as envisioned and to successfully be able to manipulate a uterus in the abdomen.

5.3 Comparison to Existing Uterine Manipulators

This section forms part of the solution to the first research questions posed in Chapter 1. It deals with the comparison of mechanical uterine manipulators to the prototype of the magnetic uterine manipulator developed in this thesis.

As per Table 5.1, it can be seen that the movement range, especially in retroversion, is inferior to that of most mechanical manipulators. This is largely due to the fact that magnetic attraction can only happen in the anterior direction of the body, whereas there is no control over forced movement in the posterior direction. Furthermore, the limited theatre space confines the arch to a rotation angle of $\pm 30^{\circ}$ from the vertical. On the other hand, the magnetic manipulator is reusable. The entire external actuator was designed with the purpose of being reused as no parts of the device have to enter the patients body. Even the internal magnet can be reused if sterilized properly. In addition, the device is able to independantly manipulate the internal magnet in two sepearate directions and it needs no assembly before operation. The actuator is simply positioned over the patient's lower abdomen during surgery preperations and the internal magnet is positioned inside the uterus.

Lastly, the cost of the magnetic manipulator is extremely competitive with the cost of the mechanical manipulators. The initial cost of the device is considerable at $\pm R15000$ ($\pm$\$1900), excluding the design work done by the author. This will be offset though by the relatively low cost of the internal magnet and housing, which will cost $\pm R300$ ($\pm$\$40). Essentially, the internal magnet and housing would be the only parts which would need replacement. Pricewise, this makes the magnetic uterine manipulator a welcome alternative to mechanical uterine manipulators. In addition, the magnetic manipulator is easy to handle and does not require training to operate. Lastly, but most importantly, the magnetic manipulator will not require any assistance as the

device can simply be operated by the surgeon and it maintains its position once moved into place, thus reducing the cost of the surgery.

In conclusion it can be said that the design and testing of the magnetic uterine manipulator was successful. Furthermore, this study proved the concept of magnetic manipulation of the uterus. The prototype device still has some shortcomings which have to be improved and there is quite a lot of room for improvement in terms of the strength and dimensions of the external magnet. Ultimately, the device will still have to be tested in vivo to properly be able to gauge the manoeuvrebility shortcomings of the magnetic manipulator.

This concludes the experimental analysis of the magnetic manipulator. The next chapter will conclude this report and act as a summary for the results obtained during the course of this thesis.

Table 5.1: Comparison of Uterine Manipulators to a Magnetic Uterine Manipulator Adapted from Mettler and Nikam (2006)

Manipulator	Movement			Reusable	Maintenance	Independant Movement	Ease of Assembly	Cost
	Anteversion / Retroversion	Lateral	Elevation					
Clermont-Ferrand	140°	130°	140°	Yes	✓✓✓	✓✓✓✓	✓	±$2500
Hohl	130°	90°	140°	Yes	✓✓	✓✓✓	✓	±$8500
Endopath	130°	90°	140°	No	✓✓	✓	✓✓	N/A
RUMI with Koh-cup	140°	90°	140°	Partially	✓✓✓	✗	✓	±$395
Hourcabie	90°	140°	140°	Yes	✓	✓✓✓✓	✓✓✓	N/A
Vcare	90°	90°	140°	No	✓✓✓	✗	✓✓✓✓	N/A
TLH-Dr Mangeshikar	130°	90°	140°	Yes	✓✓✓	✓✓	✓✓✓	±$2500
ClearView	170°	130°	140°	No	✓✓	✓✓	✓	N/A
Cohen Cannula	140°	130°	140°	No	✓✓✓	✓	✓✓	±$345
Magnetic Intra-Uterine Manipulator	60°	140°	70°	Yes	✓✓✓	✓✓✓✓	✓✓✓✓	±$1300

✗ = "Not Applicable", ✓= "Slightly Applicable", ✓✓= "Moderately Applicable", ✓✓✓= "Applicable",✓✓✓✓= "Very Applicable"

Chapter 6

Discussion

This chapter presents a discussion of the outcome of the study. Conclusions are drawn regarding the experimental as well as the numerical results. Recommendations are made for future research in this field and lessons that were learned during the course of the study are discussed. In closing, the significance of the results are discussed with respect to research in this area.

6.1 Conclusion

This section discusses the primary objective stated in Chapter 1 in context with the results obtained during this study. Four research questions were posed that directed the course of the study. This section summarizes the solutions obtained and the work done to answer the research questions.

The first research question was:

How does a magnetic manipulator compare to a mechanical uterine manipulator?

Most mechanical uterine manipulators rely on a hinge mechanism which can be rotated on the outside of the body to actuate the part which is inserted into the uterus. Thus, these devices need an assistant to manipulate the device while the surgeon focusses on the surgery. Moreover, as the device is inserted cervically and remains there for the duration of the surgery, it increases the chances of tissue trauma and cervical bleeding. A magnetic uterine manipulator on the other hand utilizes the attractive forces between two magnets to manipulate the uterus. To achieve this, a small internal magnet is inserted into the uterus and a larger external magnet is kept outside of the body. Bringing the external magnet closer to the internal magnet causes the internal magnet to attract to the external magnetic field and thus manipulate the uterus. If the external magnet is kept still, the internal magnet can be anchored in its field. The internal magnet remains in the uterus of the patient and is removed with dissection of the uterus, getting rid of moving parts that could potentially damage cervical tissue altogether. In conclusion of the first research question,

the prototype of the magnetic uterine manipulator was not able to perform the degrees of movement of existing mechanical uterine manipulators. The design compares favourably to existing systems, though. It can be reused and it does not need any extra assistance to operate. Furthermore, it does not need to be assembled and insertion of the internal magnet is simple. Lastly, the device prevents tissue damage to the cervical and vaginal canal, which benfits the patient's well-being.

The second research question was:
What type mechanical set-up is best suited for magnetic manipulation?
After an extensive literature research on existing magnetic devices that interact with the human body in a surgical environment and consultation with a gynaecologist (Dr G. Du Toit), the author can say with good certainty that the concept choice of the cart-on-arch system was the most appropriate. For the setup to be a successful candidate it had to be a simple yet elegant solution. As the operating theatre is already cluttered with equipment, the device should take up as little space as possible and should not get in the way of the surgeon. To solve this the arch system was designed not wider than 130 mm. Furthermore, it is placed directly over the uterus in the abdominal section leaving access to all the laparoscopic ports in the upper abdominal area open.

In addition, the system should be able to manipulate the uterus in a range of motion greater or at least equal to that of existing mechanical uterine manipulators. Also, the device should be easy to control. The arch design achieves a good range of motion. Lateral manipulation of the uterus is possible over an angle of 140° whereas antiversion and retroversion is possible over a range of 60°. Unfortunately, this last mentioned key design aspect is worse than that of a mechanical manipulator. The reason being the space limitations at the operating table. Any further rotation of the arch might cause dangerous interference with the surgeon. To make up for the lack of rotation, the arch design is very easy to manipulate, employing four buttons (two for each motor), to easily control the direction of rotation.

Lastly, but most importantly, the external device requires a magnet with a very high air-gap penetrating ability. The best solution for this was a rare-earth neodymium magnet. These type of magnets have a very high remnant flux density of around 1.1 - 1.4 T. In addition, they have the advantage of requiring no electricity to generate this field. It must be added though that an electromagnet with the required field strength would be a better option than the permanent magnet, for the simple reason of being switchable.

The third research question was:
What type of magnets are best suited for magnetic uterine manipulation?
This question was answered in the concept design section of this report. A perfect intra-uterine magnet requires a high field strength itself. This simplifies latching on to the external magnet flux as the two fields would compliment each other. Another requirement of the internal magnet would be self-orientation or alignment to an external field. Self-alignment would ensure that the magnet

is always positioned in a way that the force between the two magnets is always at a maximum. Rare-earth permanent magnets exhibit the highest residual flux density of any permanent magnets and were thus selected as internal magnets. To meet the self-alignment requirement, a spherical NdFeBr magnet was selected.

The final research question for this study was:
What potential safety hazards could a magnet pose in a surgical environment and how can these risks be diminished?
As described in Section 2.3.2, magnetic fields have not been linked to any major health risks or diseases since the introduction of magnets into medical devices. As described, quite a number of studies have been done which apparently show evidence of harmful effects of magnetic fields.

Despite these studies however, no other independent research has ever been able to duplicate and validate these harmful effects. In contrast, there have been numerous accounts of injuries involving magnets interfering with ferromagnetic implants or pacemakers. Thus it can be concluded, that while the effects of magnetic fields on the human body can be regarded as harmless, caution should still be taken. If magnets are brought into a surgical environment however, great care should be taken to remove any ferromagnetic objects from the surroundings and utmost care should be taken with patients who have implants or pacemakers that could be disturbed by the magnetic field.

This concludes that the research questions, posed in this thesis, were answered successfully and completely.

6.2 Recommendations for Future Research

An area of research that has not been researched in this study was the use of electromagnets as external magnets. These type of magnets were excluded from the design section as to narrow down the scope of the project. On the other hand, the extensive research study done on available electromagnets in health science research suggested that these types of magnets would be impractical to manipulate magnets over a distance since they require a high supply current or a considerable number of windings.

As discussed in the literature review, electromagnets currently in use in healthcare all require huge currents to sustain far reaching fields that are able to attract objects over a large air-gap. Also, these magnets require external cooling as the coils cannot sustain high currents for a long period of time without overheating. This would warrant research into designing electromagnets specifically tailored for large air-gap bridging, by utilizing a cooling system, employing a different core material or optimizing the coil design. To conclude, the use of an electromagnet rather than a permanent magnet would greatly enhance safety features, as the field would be able to be turned off during an emergency.

Another section that would warrant research is the design or optimization of a magnetic shield tailored to deep field generation. This study only presents a comparative simulation to depict the effects shielding has on a magnetic field. The shield affected the magnetic field of the external magnet positively by strengthening it, and the author is positive that further design optimizations could enhance the shielding. The optimization could be in the form of geometry or material selection.

Lastly, the research into methods to locate the internal magnet from the outside to establish a feedback loop and thus enable position control of the internal magnet should be done. This would give the surgeon even more control over the position of the uterus.

6.3 Significance of Research

Overall it can be said that the research presented in this thesis successfully fulfilled the research objectives. Each of the research questions posed in the introduction was successfully and methodically answered to give thorough insight into the nature of the problems at hand with a magnetic design. Furthermore, a valuable literature study was done, combining all magnetic aspects currently being employed in the health sciences and taking ideas and considerations from these studies. Thus this study can be of value to future research in the field of magnetic manipulation in health sciences.

Furthermore, to the author's knowledge, no published research has ever been done on magnets as uterine manipulators. The step by step procedure outlined in this study can give good insight into the problems involved with magnetic design involving organ manipulation and how to possibly circumvent certain problems. Lastly, the most notable contribution of this study is the research done into modelling of deep-penetrating magnetic fields which includes the setup process of the modelling software and the work done to increase the modelling accuracy of the results at large air-gaps.

List of References

Andrä, W. and Nowak, H. (1998). *Magnetism in medicine*. VCH-Verl.-Ges.

Australian Magnetic Solutions (2004). [Online] (Reviewed October 2011) Available at: `http://www.magneticsolutions.com.au/magnet-formula.html`.

Barnothy, J., Barnothy, M. and Boszormenyi-Nagy, I. (1956). Influence of a magnetic field upon the leucocytes of the mouse. *Nature*.

Berry, M. and Geim, A. (1997). Of flying frogs and levitrons. *European Journal of Physics*, vol. 18, p. 307.

Best, S. and Cadeddu, J. (2010). Use of magnetic anchoring and guidance systems to facilitate single trocar laparoscopy. *Current urology reports*, vol. 11, no. 1, pp. 29–32.

Boeckler, A., Morton, D., Ehring, C. and Setz, J. (2008). Mechanical properties of magnetic attachments for removable prostheses on teeth and implants. *Journal of Prosthodontics*, vol. 17, no. 8, pp. 608–615.

Budinger, T. *et al.* (1981). Nuclear magnetic resonance (nmr) in vivo studies: known thresholds for health effects. *Journal of computer assisted tomography*, vol. 5, no. 6, p. 800.

Buettner, U. (1992). Human interactions with ultra high fields. *Annals of the New York Academy of Sciences*, vol. 649, no. 1, pp. 59–66.

Ciuti, G., Valdastri, P., Menciassi, A. and Dario, P. (2010). Robotic magnetic steering and locomotion of capsule endoscope for diagnostic and surgical endoluminal procedures. *Robotica*, vol. 28, no. 2, pp. 199–207.

Cook, R. (1995). *Finite element modeling for stress analysis*. Wiley. ISBN 9780471107743.
Available at: `http://books.google.co.za/books?id=UyNEAQAAIAAJ`

Covens, A. and Kupets, R. (2009). *Laparoscopic surgery for gynecologic oncology*. McGraw-Hill Medical. ISBN 9780071493246.
Available at: `http://books.google.co.za/books?id=o7ITAQAAMAAJ`

Edwards, J. (2007). An introduction to magnet for static 2d modeling. Tech. Rep., Infolytica Corporation.

Eiselein, J., Boutell, H., Biggs, M. *et al.* (1961). Biological effects of magnetic fields–negative results. *Aerospace medicine*, vol. 32, p. 383.

Elkington, N. and Chou, D. (2006). A review of total laparoscopic hysterectomy: role, techniques and complications. *Current Opinion in Obstetrics and Gynecology*, vol. 18, no. 4, p. 380.

Ellis, H. and Mahadevan, V. (2010). *Clinical Anatomy: Applied Anatomy for Students and Junior Doctors*. Wiley-Blackwell.

Faddis, M. and Lindsay, B. (2003). Magnetic catheter manipulation. *Coronary artery disease*, vol. 14, no. 1, p. 25.

Grady, M., Howard III, M., Dacey Jr, R., Blume, W., Lawson, M., Werp, P. and Ritter, R. (2000). Experimental study of the magnetic stereotaxis system for catheter manipulation within the brain. *Journal of neurosurgery*, vol. 93, no. 2, pp. 282–288.

Grady, M., Howard III, M., Molloy, J., Ritter, R., Quate, E. and Gillies, G. (1990). Nonlinear magnetic stereotaxis: Three-dimensional, in vivo remote magnetic manipulation of a small object in canine brain. *Medical Physics*, vol. 17, p. 405.

Gyrus ACMI (2010). Incision points for laparoscopic hysterectomy. [Online] (Reviewed September 2010) Available at: `http://www.santafeobgyn.com`.

IBS Magnet (2007). Materials and magnet systems. Tech. Rep., Company.

IMTRONICS Institute, Thessaly, Greece (2010). Fea analysis of a human foot. [Online] (Reviewed November 2011) Available at: `http://imtronics.cereteth.gr/?p=528`.

Integrated Magnetics (2011). [Online] (Reviewed October 2011) Available at: `http://www.intemag.com/faqs.html`.

Kavic, M. and Levinson, C. (1999). *Prevention & management of laparoendoscopic surgical complications*. Society of Laparoendoscopic Surgeons. ISBN 9780966376807.
Available at: `http://books.google.co.za/books?id=-B6qGq8WThQC`

Klitzing, L. (1986). Do static magnetic fields of nmr influence biological signals? *Clinical Physics and Physiological Measurement*, vol. 7, p. 157.

Kume, M., Miyazawa, H., Iwasaki, W., Abe, F., Uchinami, H. and Yamamoto, Y. (2008). The use of magnetic anchors in the bowel lumen for laparoscopic anterior resection of rectosigmoid colon in pigs: with video. *World journal of surgery*, vol. 32, no. 11, pp. 2425–2428.

Martini, F., Bartholomew, E., Ober, W., Garrison, C., Welch, K. and Hutchings, R. (2000). *Essentials of anatomy & physiology*. Prentice Hall.

Meeker, D., Maslen, E., Ritter, R. and Creighton, F. (1996). Optimal realization of arbitrary forces in a magnetic stereotaxis system. *Magnetics, IEEE Transactions on*, vol. 32, no. 2, pp. 320–328.

Merz, E., Miric-Tesanic, D., Bahlmann, F., Weber, G. and Wellek, S. (1996). Sonographic size of uterus and ovaries in pre-and postmenopausal women. *Ultrasound in Obstetrics & Gynecology*, vol. 7, no. 1, pp. 38–42.

Mettler, L. and Nikam, Y. (2006). A comparative survey of various uterine manipulators used in operative laparoscopy. *Gynecological Surgery*, vol. 3, no. 4, pp. 239–243.

Mettler, L., Sammur, W. and Schollmeyer, T. (2010). Hysterectomy for uterine disease in 2010: from past to future. *Clinical Medicine Insights: Reproductive Health*, vol. 4, no. 1, pp. 7–22.

Moore, P. (2005). Mri-guided congenital cardiac catheterization and intervention: The future? *Catheterization and cardiovascular interventions*, vol. 66, no. 1, pp. 1–8.

Parker, R. (1990). *Advances in permanent magnetism*. AWiley interscience publication. Wiley. ISBN 9780471822936.
Available at: `http://books.google.com/books?id=5sBnQgAACAAJ`

Raman, J., Scott, D. and Cadeddu, J. (2009). Role of magnetic anchors during laparoendoscopic single site surgery and notes. *Journal of Endourology*, vol. 23, no. 5, pp. 781–786.

Rizzoni, G. (2007). *Principles and Applications of Electrical Engineering*. McGraw-Hill Higher Education. ISBN 9780071254441.
Available at: `http://books.google.co.za/books?id=fgPxQwAACAAJ`

Schenck, J. (2000). Safety of strong, static magnetic fields. *Journal of Magnetic Resonance Imaging*, vol. 12, no. 1, pp. 2–19.

Schenck, J. *et al.* (1996). The role of magnetic susceptibility in magnetic resonance imaging: Mri magnetic compatibility of the first and second kinds. *MEDICAL PHYSICS-LANCASTER PA-*, vol. 23, pp. 815–850.

Sculpher, M., Manca, A., Abbott, J., Fountain, J., Mason, S. and Garry, R. (2004). Cost effectiveness analysis of laparoscopic hysterectomy compared with standard hysterectomy: results from a randomised trial. *Bmj*, vol. 328, no. 7432, p. 134.

Shirazee, N. and Basak, A. (1995). Electropermanent suspension system for acquiring large air-gaps to suspend loads. *Magnetics, IEEE Transactions on*, vol. 31, no. 6, pp. 4193–4195.

Sutton, C. (1997). Hysterectomy: A historical perspective. *Baillière's clinical obstetrics and gynaecology*, vol. 11, no. 1, pp. 1–22.

Swain, P., Toor, A., Volke, F., Keller, J., Gerber, J., Rabinovitz, E. and Rothstein, R. (2010). Remote magnetic manipulation of a wireless capsule endoscope in the esophagus and stomach of humans (with videos). *Gastrointestinal endoscopy*, vol. 71, no. 7, pp. 1290–1293.

Wang, X. and Meng, M. (2007). A magnetic stereo-actuation mechanism for active capsule endoscope. In: *Engineering in Medicine and Biology Society, 2007. EMBS 2007. 29th Annual International Conference of the IEEE*, pp. 2811–2814. IEEE.

Wijeysundera, D., Beattie, W., Austin, P., Hux, J. and Laupacis, A. (2010). Non-invasive cardiac stress testing before elective major non-cardiac surgery: population based cohort study. *BMJ: British Medical Journal*, vol. 340.

Xu, Z., Jin, N., Shi, L. and Xu, S. (2004). Maglev system with hybrid-excited magnets and an air-gap length control. In: *Maglev*, vol. 2, pp. 1019–1023.

Appendices

Appendix A

Appendix A - Anatomical Reference Planes

Medical professionals often refer to body parts in terms of anatomical planes. These imaginary planes dissect the body at certain physiologically distinct areas or in planes of symmetry. Figure A.1 depicts the anatomical planes.

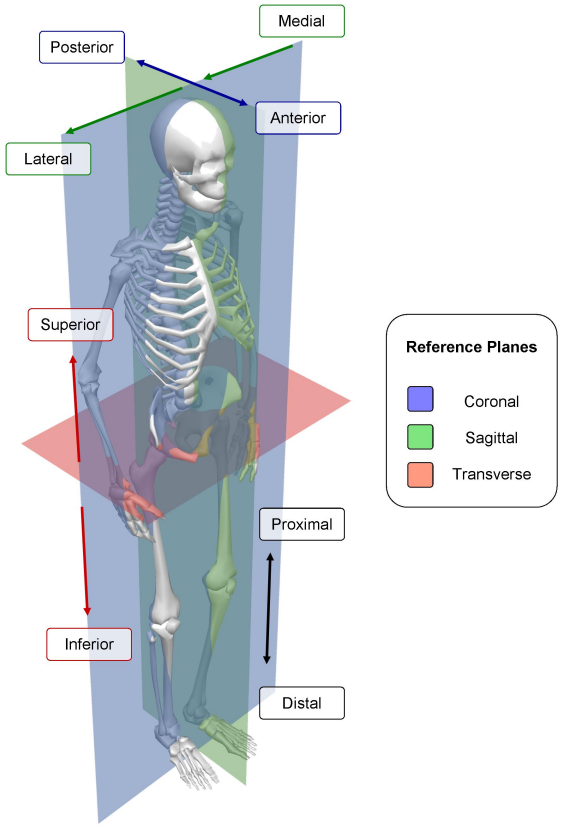

Figure A.1: Anatomical Reference Planes (Image: J. vd. Merwe)

Appendix B

Appendix B - Rare-Earth Permanent Magnet Comparison

Table B.1 presents the most common rare-earth magnets arranged from strongest to weakest. This table was used to select the internal and external magnet types. The residual flux density determines the strength of the magnet.

Table B.1: Table of rare earth magnets (Integrated Magnetics, 2011)

	Maximum Energy Product *Bhmax(MGOe)*	Residual Flux Density *Br(G)*	Coercive Force *Hc(Koe)*	Working Temperature *°C*
Ceramic 5	3.4	3950	2400	400
Sintered Alnico 5	3.9	10900	620	540
Cast Alnico 8	5.3	8200	1650	540
Samarium Cobalt 20 (1,5)	20	9000	8000	260
Samarium Cobalt 28 (2,17)	28	10500	9500	350
Neodymium N45	45	13500	10800	80
Neodymium 33UH	33	11500	10700	180